PROCEEDINGS A

rspa.royalsocietypublishing.org

Invited Review

Check for updates

Article submitted to journal

Subject Areas:
Solar Physics, Plasma Physics, Space Science

Keywords:
Flares, Coronal Mass Ejections, Magnetic Fields, Filaments/Prominences, Solar Energetic Particles, Magnetic Reconnection, Magnetohydrodynamic Simulation

Author for correspondence:
Yuandeng Shen
e-mail: ydshen@ynao.ac.cn

THE ROYAL SOCIETY PUBLISHING

Observation and Modeling of Solar Jets

Yuandeng Shen[1]

[1]Yunnan Observatories, Chinese Academy of Sciences, Kunming, 650216, China

The solar atmosphere is full of complicated transients manifesting the reconfiguration of solar magnetic field and plasma. Solar jets represent collimated, beam-like plasma ejections; they are ubiquitous in the solar atmosphere and important for the understanding of solar activities at different scales, magnetic reconnection process, particle acceleration, coronal heating, solar wind acceleration, as well as other related phenomena. Recent high spatiotemporal resolution, wide-temperature coverage, spectroscopic, and stereoscopic observations taken by ground-based and space-borne solar telescopes have revealed many valuable new clues to restrict the development of theoretical models. This review aims at providing the reader with the main observational characteristics of solar jets, physical interpretations and models, as well as unsolved outstanding questions in future studies.

1. Introduction

The dynamic solar atmosphere hosts many jetting phenomena that manifest as collimated plasma beams with a width ranging from several hundred to few times 10^5 km [1–5]; they are frequently accompanied by micro-flares, photospheric magnetic flux cancellations, and type III radio bursts, and can occur in all types of solar regions including active regions, coronal holes, and quiet-Sun regions. Since these jetting activities continuously supply mass and energy into the upper atmosphere, they are thought to be one of the important source for heating coronal plasma and accelerating solar wind [1,6–9].

This review mainly focuses on bigger solar jets including surges, coronal jets, and macro-spicules. Although these jet activities are observed at different scale and temperature range, they can be viewed as the same type of solar jets due to their similar observational characteristic and generation mechanism, i.e., magnetic reconnection dominated jet-like activities with an inverted-Y structure. For smaller, lower-energy jet-like activities like spicules and dynamic fibrils, their

generation mechanisms are still open questions. Previous studies suggested that spicules and dynamic fibrils are possibly launched by upward propagating shocked pressure-driven waves leaking from the photosphere [10,11]. However, some recent studies indicated that a portion of spicules are possibly produced by the same mechanism resembling bigger jets, since they also showed an inverted-Y shape and associated with flux cancellations [9,12,13]. Hence, the generation of these small jet-like activities needs further investigation, and the present review will not introduce them in detail. Readers who are interested in this topic can refer to several previous reviews [14–16].

The observation of solar jets can date back to 1940s; they were dubbed surges in history [17]. At the very beginning, surges were found to be associated with micro-flares or sudden brightenings near their footpoints [18]. Afterwards, observations suggested that surges were dominated by local magnetic fields [19]; they move along magnetic field lines and tend to occur above satellite sunspots or in regions of evolving magnetic features [20,21]. Before 1990s, observations were mainly taken by small-aperture ground-based Hα telescopes and a few low-resolution space instruments such as the *Skylab* (1991-2001) and *SMM* (1980-1989). Solar jets were studied intensively since 1990s due to the launch of a series of space telescopes, including the *Yohkoh* satellite [22], the *Solar and Heliospheric Observatory* [23] (*SOHO*; 1995 to now), the *Transition Region and Coronal Explorer* [24] (*TRACE*; 1998-2010), the *Reuven Ramaty High Energy Solar Spectroscopic Imager* [25] (*RHESSI*; 2002-2018), the *Hinode* [26] (2006 to now), the *Solar Terrestrial Relations Observatory* [27] (*STEREO*; 2006 to now), the *Solar Dynamics Observatory* [28] (*SDO*; 2010 to now), and the *Interface Region Imaging Spectrograph* [29] (*IRIS*; 2013 to now). In the meantime, more and more ground-based large-aperture solar telescopes were put into routine observation, for example, the Swedish Solar Telescope [30] (SST; 1-meter), the Goode Solar Telescope [31] (GST; 1.6-meter), and the New Vacuum Solar Telescope [32] (NVST; 1-meter). So far, the temporal (spatial size) resolution has been largely improved from tens of minutes (several arcseconds) to a few seconds (sub-arcsecond), and we now observe the Sun from multiple view angles with imaging and spectroscopic instruments covering a broad waveband from radio to hard X-ray (HXR). The current high spatiotemporal resolution imaging, spectroscopic, and stereoscopic observations continuously increase our knowledge about solar jets. In addition, due to the tremendous improvement of computing power and calculation techniques, numerical modeling of solar jets has also achieved great progress in recent years. Nowadays, the study of solar jets has become a main research field in solar physics.

Over the past three decades, significant advances achieved in observational, theoretical, and numerical analyses have contributed to shaping our evolving understanding of the different aspects of solar jets, such as their triggering and driving mechanisms, fine structures, and their relationship with other solar activities [33]. Now, we recognize that the basic energy release mechanism in solar jets is magnetic reconnection, which converts magnetic free energy into kinetic energy, thermal energy, and radiant energy of particles [34,35]. Recent high spatiotemporal resolution observations showed that solar jets are probably miniature version of large-scale eruptions such as filament eruptions and coronal mass ejections (CME) [36,37]. In addition, recent ultrahigh resolution observations further indicated that the eruption of small spicules is possibly the same as solar jets, since they were evidenced to be associated magnetic flux cancellations and possibly mini-filament eruptions in several observational studies [9,13,38,39]. Therefore, these results may suggest a scale invariance of solar eruptions, and our understanding of solar jets can probably be applied to interpret the complicated and energetic large-scale solar eruptions and currently unresolved small spicules. Solar jets are also important for space weather forecasting, because they often eject large-scale mass and energetic particles into the interplanetary space.

Despite the great progress achieved in the past, the detailed physics behind solar jets is still not completely understood. For example, questions about their triggering and driving mechanisms, evolution behaviors, fine structures, and particle acceleration; how do small-scale solar jets evolve into large-scale CMEs? how do they contribute to coronal heating and solar wind acceleration? In addition, whether different jetting phenomena from the photosphere to the low corona are

interconnected, or are they driven by the same mechanism but different emission components of the same basic physical process? Could the current models of solar jets be applied to explain small spicules and large filament/CME eruptions? The main aim of this review is to summarize our current knowledge of solar jets, and attempt to discuss how close we are to the answers to the above questions. Readers who are interested in the relevant research fields can refer to several previous reviews [16,33,40–42].

2. Observational Feature

(a) Morphology and Classification

Solar jets are generally described as collimated, beam-like ejecting plasma flows along straight or slightly oblique magnetic field lines. Due to the huge improvement of the observing capabilities, solar jets can be imaged in a wide temperature range from the photosphere to the outer corona. According to different classified methods, solar jets were classified into different types in history. Firstly, solar jets were divided into photospheric jets, chromospheric jets (or surges), transition region jets, coronal jets, and white-light jets, based on the temperature of the atmosphere in which they occur. Secondly, they were classified as coronal hole jets, active region jets, and quiet-Sun region jets, based on regions where they occur. Thirdly, they were classified as Hα jets, extreme ultraviolet (EUV) jets, and X-ray jets, depending on different observing wavebands. Nevertheless, since solar jets are often observed simultaneously at different wavebands covering a wide temperature range, and they can occur in all types of solar regions, it seems that the above classified methods are not very reasonable if one considers the physical properties and morphologies.

Based on morphology, Shibata et al. [44] classified coronal jets into straight anemone jets and two-sided-loop jets (see Figure 1). An anemone jet exhibits as an inverted-Y shape consisting of a straight plasma beam and a bright dome-like base. In contrast, a two-sided-loop jet appears as a pair of plasma beams ejecting in opposite directions from the eruption source region [43,45–49]. Recently, high resolution observations combined with extrapolated three-dimensional (3D) coronal magnetic fields together revealed the fan-spine topology magnetic system of straight anemone jets [50], which consists of a coronal nullpoint, a dome-like fan that represents the closed separatrix surface, and inner and outer spines belonging to different connectivity domains [51–60]. A fan-spine topology often arises when a parasitic magnetic polarity emerges (or carries) into a preexisting magnetic field region with opposite polarity, and a jet occurring within it can lead to three flare ribbons due to the low-altitude impact of particle beams accelerated through the

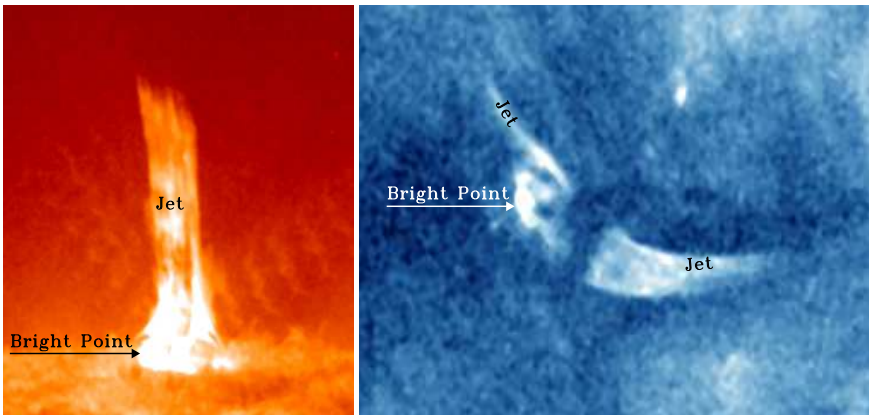

Figure 1. *SDO*/AIA 304 Å (left) and 335 Å (right) images show an anemone jet on 2015 January 30 and a two-sided-loop jet on 2013 June 02 [43], respectively. The arrows indicate the bright points in the eruption source regions.

nullpoint magnetic reconnection, namely, an inner bright patch surrounded by a circular ribbon relevant to the inner spine and the dome-like fan structure, and a remote elongated bright ribbon associated with the outer spine. In principle, the fan-spine topology represents the 3D magnetic structure of all straight anemone jets. For straight jets in coronal hole, their outer spines are very long and can be regarded as open fields in the outer corona; therefore, their remote footpoints (brightenings) of the outer spines can not be identified, and these jets can be considered as eruptive jets. In comparison, for straight jets in or around active regions, one can often identify their entire fan-spine structures due to their shorter outer spines. For these jets, they can be considered as confined jets, because their ejecting material is typically observed to be confined within the fan-spine system. Straight anemone jets could be further divided into inverted-Y and λ types, in which an inverted-Y (λ) type jet was commonly interpreted as a small-scale magnetic bipole reconnecting with the ambient open coronal magnetic fields around the bipole top (footpoint). Hence, the different shapes could possibly be used to distinguish the reconnection sites in solar jets [61].

Moore et al. [63] classified straight anemone jets into standard jets and blowout jets based on their different physical properties. According to their definition, blowout jets exhibited several different distinguishing characteristics relative to standard jets that are the same as typical anemone jets, including 1) an additional brighten point inside the base arch besides the outside one, 2) the blowout eruption of the base arch that often host a twisting mini-filament, and 3) and extra jet-spire strand rooted close to the outside bright point (see Figure 2). At the beginning, Moore et al [63] found that about two (one) third anemone jets belong to standard (blowout) type

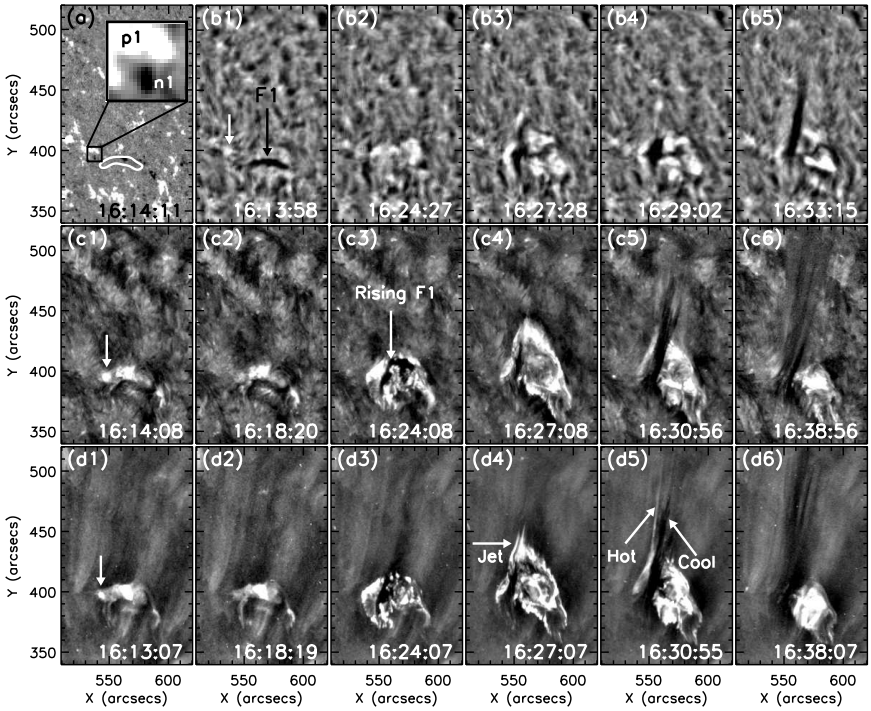

Figure 2. An example of blowout jets [62]. (a) is a *SDO*/HMI magnetogram, in which the inset shows a small bipole near the left end of the mini-filament (white contour). (b1)–(b5) are Hα images from Big Bear Solar Observatory. (c1)–(c6) and (d1)–(d6) are *SDO*/AIA 304 Å and 193 Å images, respectively. The white arrows in (b1), (c1), and (d1) point to a bright patch at the location of the small bipole prior to the jet. The black arrow in (b1) and the one in (c3) indicate the pre-eruption and rising phases of the mini-filament, respectively. The arrow in (d4) indicates the first appearance of the hot jet, and the two arrows in (d5) point to the jet's hot and cool components, respectively.

jets; however, this result was then updated to be about 50% each when the statistical samples were expanded [64]. Sterling et al. [36] studied 20 polar jets and proposed that all jets are generated in the same way as blowout jets; they argued that the successful (failed) eruptions of the mini-filaments inside the base arches can account for the observational characteristics of blowout (standard) jets. In a subsequent paper, Moore et al. [65] further examined 15 of the 20 jets studied by Sterling et al. [36] to study the onset of the magnetic explosion in polar coronal jets; they found that a large majority of polar jets work the same way as large-scale magnetic breakout eruptions in association with energetic flares and CMEs, in which external breakout reconnection proceeds and is involved in the triggering of the eruption. Taken together with the results of Panesar et al. [66–68] they also claim that flux cancellation is the main process whereby the energy is stored prior to eruption in all jets and CMEs, and may also be involved in the triggering process. So far, the finding of blowout jets has been confirmed by many observational studies, and now we recognized that the vast majority of solar jets are caused by magnetic flux cancellation rather than flux emergence [62,69–84]. Recently, high resolution observational studies showed that two-sided-loop jets are also associated with flux cancellations and include the eruption of mini-filaments inside the base arches [43,46,49,85,86], and two-sided-loop jets occurring in filament channels may important for causing the eruption of large filaments [87].

(b) Precursor

Solar jets are evidenced to be launched from various pre-eruption structures including satellite sunspots (or small opposite-polarity magnetic elements), mini-filaments, coronal bright points, and mini-sigmoids. Observationally, these structures can be regarded as the progenitor of solar jets, and studying of them can contribute to the prediction of the occurrence and evolution characteristics of solar jets.

In the photosphere, satellite sunspots can be considered as a conspicuous progenitor for surges or many active region coronal jets. Rust [20] reported that surges are liable to occur at nullpoints above satellite sunspots. Roy [21] confirmed this finding and further proposed that significant magnetic flux change over a short time interval is also important for producing surges. Subsequent studies based on high resolution observations revealed that the appearance of evolving satellite sunspots are liable to launch recurrent jets through continuously collision with the main sunspots [55,88–94]. In quiet-Sun and coronal hole regions, small opposite-polarity magnetic elements can be recognized as the most conspicuous photospheric progenitor for many lower-energy, small-scale coronal jets. Generally, observations suggest that the onset of these jets are often tightly associated with magnetic flux cancellations caused by the converging and/or shearing motions of the magnetic elements' opposite polarities [62,65,66,68].

Mini-filaments in the chromosphere and the corona can be recognized as an important progenitor for producing coronal jets. Mini-filaments were found to be eruptive in nature, and their eruption characteristics are similar to those evidenced in large-scale filament eruptions [95]. Several earlier observations showed that mini-filament eruptions are tightly associated with coronal jets; however, the authors did not clarify the physical relationship between them [89,96]. Shen et al. [62,69] studied two blowout jets and found that the erupting mini-filaments directly form the cool component of coronal jets (see Figure 2). Recently, more and more observational studies confirmed that blowout jets are driven by mini-filament eruptions or filament channels [73–84,97,98]; some authors even proposed that all coronal jets are originated from mini-filament eruptions, and their generation resembles the eruption of large-scale, energetic filament/CME eruptions [36,65,99].

Solar jets are frequently observed to be ejected from coronal bright points and micro-sigmoids. Coronal bright points represent a set of small-scale low-corona loops with enhanced emission in the EUV and X-ray spectra [101,102], and plasma ejections were found to be originated from them [6,103,104]. Recent high resolution observations showed that coronal bright points are ubiquitous in the corona [105], and they are found to be liable to produce solar jets [106–109]. Statistical studies indicated that a majority of coronal bright points produce at least one eruption during

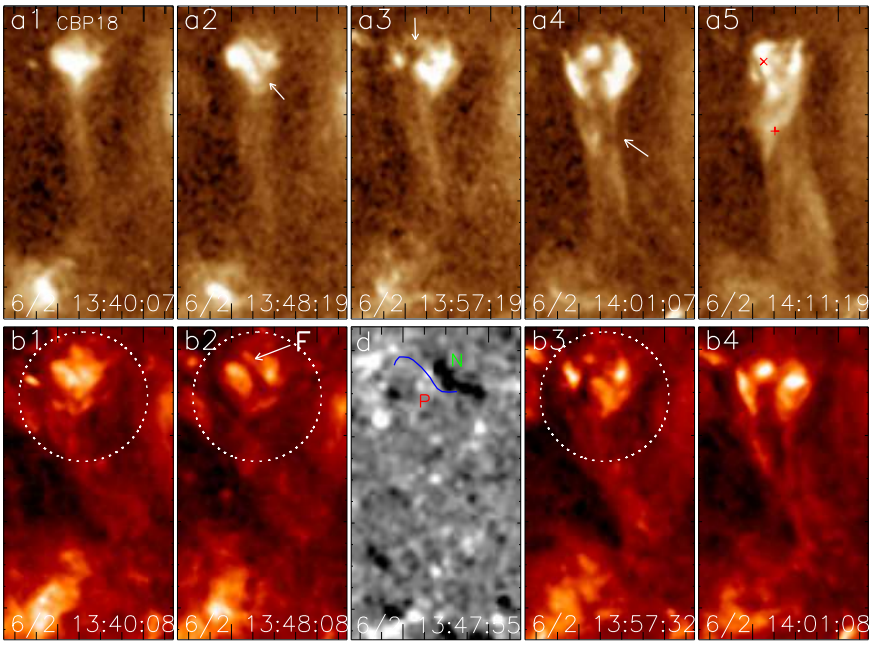

Figure 3. Examples of solar jets originated from EUV bright points [74] (top and middle rows) and mini-sigmoid structures [100] (bottom row). (a1)–(a5), (b1)–(b4), and (d) are *SDO*/AIA 193 Å, 304 Å, and magnetogram images, respectively. A mini-filament is indicated by the arrows in (a2) and (b2), and the jet spire is indicated by the arrow in (a4). The circles mark the bright point region. The blue curve in (d) indicate the position of the mini-filament on the magnetogram. (i)–(l) are *Hinode* soft X-ray images from the *Hinode*.

their lifetime (≈21 hours) [110]. Hong et al. [74] found that about one quarter to one third of coronal bright points produce one or more filament-driven blowout jets during their lifetimes (see the top and middle panels of Figure 3).

A coronal sigmoid consists of many differently oriented loops that all together form two opposite J-shaped bundles or an overall S-shaped structure [111], which is more likely to be eruptive and is a main progenitor of solar eruptions [112]. Micro-sigmoids have a typical size of about one fifth of the large-scale ones; they can be formed through injecting twist into simple coronal bright points [113], or via tether-cutting reconnection mechanism [109]. Using the *Hinode* X-ray observations, Raouafi et al. [100] identified that some coronal jets are evolved from mini-sigmoids (see the bottom panels of Figure 3). Liu et al. [114] reported a special case in which a pair of twin blowout jets were successively generated from a sigmoid structure; the authors proposed that the two jets were produced by the reconnection between the ambient open fields and the two opposite J-shaped twisted sigmoidal magnetic fluxes, respectively. These observations indicate that coronal mini-sigmoids can be recognized as a progenitor of coronal jets [100].

(c) Fine Structure

(i) Cool and Hot Components

Sometimes, cool and hot plasma flows can be identified simultaneously in a single jet. The co-existed cool and hot components can be observed in EUV images, or separately appear in Hα images as a surge and in EUV or soft X-ray images as a coronal jet [62,69,88,115–117]. Some earlier studies indicated that the cool and hot components of solar jets are correlated in time and space, and with similar kinematic behaviors [118–120]. The cospatial relationship was confirmed by some recent high spatiotemporal resolution observations [121], although the two components were not exactly cospatial over the entire length [115], or the hot component had a higher speed than the cool one [122]. Nevertheless, the two components of soar jets were also found to be adjacent to each other in some events [62,69,88,96,117,123,124]. Particularly, Chae et al. [123] reported several jets whose hot EUV components were identified with the cool Hα bright jet-like features. Jiang et al. [117] studied three jets whose cool and hot components showed different evolutions not only in space but also in time, in which the cool Hα component had a smaller size than the larger, hot one, and the former moved along the edges of the latter.

The appearance of the cool component in a jet is often after the corresponding hot one a few minutes [62,69,115,117,125–127]. Specially, in the outer corona at a height of 1.71 $R_\odot$, Dobrzycka et al. [128] observed 5 polar jets in which the arriving of cool components were after the hot ones about 25 minutes. There is one case in which the cool component (surge) appeared about 2 hours before the corresponding hot X-ray jet [90]. This abnormal result was probably caused by the unsteady cadence and low spatial resolution of the *Yohkoh* X-ray data. Since solar jets can occur repeatedly from the same source region, and their lifetimes are usually of 40 minutes or less according to high resolution observations, the 2 hours time interval seems too long for a single jet. Hence, the cool surge and the hot X-ray jet in Zhang et al. [90] were very possibly two different jets originated from the same source region, rather than simultaneous cool and hot components in a single jet.

The different spatial relationships can possibly be reconciled by considering the projection effect. In principle, observational results suggested that the two components are along different magnetic field lines and dynamically connected. Therefore, their spatial relationship should be not cospatial but adjacent to each other. The cospatial case can be expected when the two components are overlapped to each other along the line-of-sight. For the delayed appearance of the cool component, one can understand it based on the formation mechanism of solar jets. Previously, the delayed appearance of the cool component was explained as the cooling of the earlier, hotter one [115,117,125], the emerging chromospheric or transition region cool plasma accelerated magnetic tension force of the newly formed magnetic reconnection field lines [123,127,129], or the different Alfvén speeds in the cool (high-density, low Alfvén speed) and hot (low-density, high Alfvén speed) plasma flows [130]. Based on high spatiotemporal resolution observations (see Figure 2(d5)), several works provide evidence that the cool component of jets is directly formed by the erupting mini-filaments confined within the jet base [36,38,39,43,62–64,69, 74,110,131]. According to the interpretation of Shen et al. [43,62,69], a mini-filament is confined by a small arch surrounded by open field lines. Due to some reasons, the arch starts to reconnect with the ambient open field lines (external reconnection), which produces the hot jet component like the generation of a standard jet. The external reconnection not only produces the hot jet but also removes the confining field lines of the mini-filament, which further results in the instability and eruption of the filament due to the internal reconnection between the two legs of the confining field lines. Therefore, the appearance of the cool component is naturally after the hot one, and their spatial relationship is adjacent to each other. So far, more and more observations indicated the appearance of cool component in solar jets, especially in blowout jets that often involve the eruption of mini-filaments [36,38,39,63,64,74,110,131].

(ii) Plasmoid

Supported by various observational evidences [40], it has been widely accepted that solar jets are produced by magnetic reconnection [33]. A typical evidence supporting the reconnection scenario

is the formation and ejection of outward plasmoids (also called magnetic islands, or plasma blobs) due to tearing-mode instability of the current sheets. Singh et al. [132] observed multiple bright plasmoids in several jets imaged by the Ca II *H* filtergram of the *Hinode*/SOT, whose typical lifetime, size, and intensity enhancement relative to the background are about 20–60 seconds and 0.3–1.5 Mm, and 30%, respectively. Plasmoids has a multi-thermal (1.4–3.4 MK) structure with a number density in the range of $1.7 - 2.89 \times 10^{10}$ cm^{-3} [69,133,134]. Subarcsecond plasmoids were detected by the *IRIS*, whose average size is about 0.57 Mm, and their ejecting speed ranges from 10 to 220 km s^{-1} [135]. Besides the observation of plasmoids in straight anemone jets [81,136–139], they were also observed in two-sided-loop jets [43] (see Figure 4). Analysis results indicated that plasmoids observed in different types of jets were similar, and they were thought to be created by magnetic reconnection as a result of tearing instability of the current sheets.

Numerical experiments also revealed the appearance of plasmoids in solar jets. Yokoyama & Shibata [129,140] performed the two-dimensional (2D) simulations of solar jets, in which they evidenced the creation, coalesce, and ejection of plasmoids in the current sheets. In another simulation, high-temperature and high-density plasmoids were generated repeatedly at the same location and were ejected upward and downward simultaneously [141]. The authors claimed that the merged upward moving plasmoids correspond to the anemone jets as in observations. Ni et al. [142,143] tested the low and high plasma β cases to study the formation of plasmoids in solar jets; they found that plasmoids with similar characteristic parameters as in observations are easily created in the low β case, while the high β case created vortex-like structures due to Kelvin-Helmholtz (KH) instability. According to this study, the observed discrete high density features in solar jets could either be plasmoids or vortex structures at different wavebands. In 3D simulations, plasmoids were evidenced as twisted flux ropes resembling the shape of solenoids, and they are formed most likely the result of resistive tearing mode instabilities in the current sheets located between closed and open fields [144,145]. Wyper et al. [146] pointed out the tearing process should occur at the separatrix surface between the closed and open flux systems, and the repeated formation and ejection of flux ropes can naturally explain the intermittent outflows, bright blobs, and filamentary structure observed in some jets.

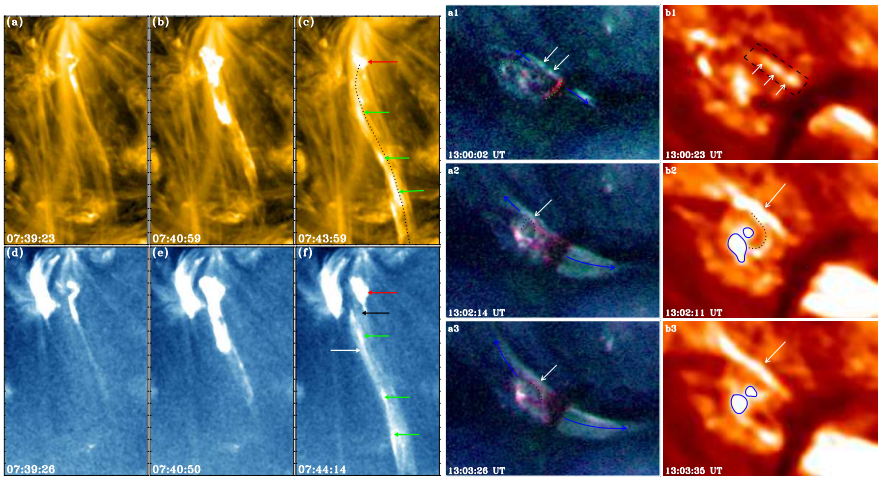

Figure 4. Examples of plasmoids in anemone [69] (left three columns) and two-sided-loop jets [43] (right two columns). The anemone jet is displayed with the *SDO* 171 Å (top row) and 335 Å (bottom row) images, in which the green arrows indicate the plasmoids along the jet spire. The two-sided-loop jet is shown with the *SDO* composite high-temperature images made from the AIA 94 Å (red), 335 Å (green), and 193 Å (blue) channels (left column) and the 304 Å (right column) images. The arrows in the top row point to the plasmoids in the current sheet, while those in the middle and bottom rows indicate the current sheet.

(iii) Kelvin-Helmholtz Instability

KH instability is a basic physical process that occurs when there is velocity shear in a single continuous fluid, or where there is a velocity difference across the interface between two fluids [147]. Recent observations revealed the occurrence of KH instability in the solar atmosphere, such as at the interface between erupting region and the surrounding corona [148], at the outer edge of CMEs [149], in prominences [150], in coronal streamer [151], and in solar jets [152,153].

Vortex structures caused by KH instability can be regarded as a basic fine structure of solar jets, which were frequently observed within or at the outer edge of solar jets [154,155]. Using *IRIS* observations, Li et al. [152] reported the developing process of KH instability in a blowout jet due to the strong velocity shear of two plasma flows along the jet spire, in which the developing process was about 80 seconds, and the distortion scale was less than 1.6 Mm. Using Hα observations taken by the NVST, Yuan et al. [153] studied the KH instability at the outer edge of a small solar jet, in which the KH instability was thought to be caused by the shearing motion between cool chromospheric and hot coronal plasma flows. During the mature stage, plasma heating was evidenced around the region of the vortex structures, supporting the scenario that KH instability can effectively transfer plasma kinetic energy into thermal energy and heat the coronal plasma. Since velocity shear can occur at a variety of length scales and different regions in the solar atmosphere, this finding led the authors to conjecture that KH instability could be an effective way to supply energy to heat the corona plasma.

Theoretical and numerical works were performed to study the KH instability in rotating solar jets. Zaqarashvili et al. [156] found that rotating jets are unstable to KH instability when the kinetic energy of rotation is more than the magnetic energy of the twist; the growth time of KH instability is several seconds for miniature jet-like events and a few minutes or less for large jets. The authors argued that rotating jets may provide energy for chromospheric and coronal heating, since KH vortices can lead to enhanced turbulence development and heating of the surrounding plasma.

(d) Dynamical Characteristic

(i) General Property

Based on *Yohkoh* soft X-ray observations, Shimojo et al. [157] concluded several typical properties of X-ray jets, including that 1) most of jets are associated with micro-flares whose brightest parts show a gap between the exact footpoints of the jets; 2) the lengths (widths) are in the range of a few $\times 10^4$–4×10^5 (5×10^3–10^5) km; 3) the apparent velocities are of 10 to 1000 km s^{-1} with a mean value of about 200 km s^{-1}; 4) the distribution of the lifetimes is a power law with an index of about 1.2; 5) most active region jets are observed to the west of the active regions; 6) 76% jets show constant or converging spires whose widths get narrower from the photosphere to the corona, and their intensity distribution often show an exponential decrease with distance from the footpoints. In a subsequent paper [4], they further concluded that 1) the temperatures of the jets are 3–8 MK with an average value of 5.6 MK, similar to those of the associate flares, and it shows a correlation with the sizes of the associated flares; 2) the density is in the range of 0.7–4.0$\times 10^9$ cm^{-3} with an average value of 1.7×10^9 cm^{-3}; 3) the thermal energies of the jets are $10^{27} - 10^{29}$ ergs, far less than those of the associated flares; and 4) the apparent velocity of the jets is usually slower than the sound speed. The physical parameters were further studied based on a large sample of 7197 coronal hole X-ray jets observed by the *Hinode* [158], the authors found that the peaked distributions with maxima of the outward velocities, the lengths, widths, and lifetimes of the jets are 160 km s^{-1}, 5×10^4 km, 8×10^3 km, and 10 minutes, respectively. In addition, the velocities of transverse motions perpendicular to the jet axis are ranged from 0–35 km s^{-1}.

Using Ca II *H* broadband filter observations taken by the *Hinode*/SOT, Nishizuka et al. [159] made a statistically study of chromospheric anemone jets [1]. Different from spicules [15,16] and dynamic fibrils [160], this type of jets are usually observed in active regions and show bright cusp-like or inverted Y-shaped structures, and are smaller and occur much more frequently than

surges. The authors found that the shape of chromospheric anemone jets are similar to X-ray jets, suggesting their common formation mechanism. The typical parameters of lengths, widths, lifetimes, and velocities of chromospheric anemone jets are in the ranges of about 1–4 Mm, 100–400 km, 100–500 seconds, and 5–20 km s^{-1}, respectively. In addition, the velocities are found to be comparable to the local Alfvén speed in the lower solar chromosphere.

Nisticó et al. [61] performed a statistically study of energetic polar EUV jets using *STEREO* observations; they found that the appearance of EUV jets are always correlated with small-scale chromospheric bright points. The typical lifetimes of the studied EUV jets are 20 (30) minutes at 171 (304) Å while that of the white-light jets observed in coronagraph are peaked at around 70–80 minutes. It was found that the speeds are 400 and 270 km s^{-1} for the hot 171 Å and cool 304 Å components, respectively. The speeds measured from 171 Å observations are comparable to those derived from coronagraph observations (390 km s^{-1}). Mulay et al. [161] studied active region EUV jets observed by the *SDO*, their results indicated that the lifetimes and velocities are in the ranges of 5–39 minutes and 87–532 km s^{-1}, and the corresponding average values are 18 minutes and 271 km s^{-1}, respectively. Typically, all the studied jets were co-temporally associated with Hα jets and nonthermal type III radio bursts, and 50% (30%) events in their samples were originated in regions of flux cancellation (emergence). Other similar statistical studies based on *STEREO* and *SDO* observations can also be found in the literature [162,163]. In statistical studies of white-light jets based on coronagraphs onboard the *SOHO*, the speeds of jets at solar minimum of activity are in the range of 400 to 1100 km s^{-1} for the leading edge and 250 km s^{-1} for the bulk of their material, while the typical speeds at maximum of activity are around 600 km s^{-1} [164,165]. In addition, Kiss et al. [166] statistically studied 301 macrospicular jets using the AIA 304 Å observations from 2010 June to 2015 December. The authors found a strong asymmetry in the spatial distribution in terms of solar north/south hemispheres, and the average lifetime, width, length, and velocity of the studied macrospicular jets are 16.75 ± 4.5 minute, 6.1 ± 4 Mm, 28.05 ± 7.67 Mm, and 73.14 ± 25.92 km s^{-1}, respectively.

(ii) Rotating Motion

Rotating motion is a typical dynamical characteristic of solar jets. Earlier observations evidenced the appearance of rotating motion in prominences like a tornado [167–169], and this kind of motion is frequently evidenced in erupting filaments [170–176]. Xu et al. [177] detected the rotating motion in a surge using the Hα spectral observations. With the improvement of the quality of imaging and spectral observations, rotating motion was widely observed in Hα surges [90,178,179], EUV jets [2,88,115,117,180,181], and macrospicules [182,183]. Some observations suggested that the eruption of twisted filaments sometime show as rotating jets [84,174,184], and it can be explained as a result of the reconnection between twisted filaments and their surrounding open fields [185]. In such a process, the magnetic twist stored in the closed filaments or loops are released into open magnetic fields, and plasma is driven out in the relaxation process [2,88,179].

Stereoscopic observations taken by *STEREO* imaged the fine helical structure of rotating jets, which exhibited different morphologies when they are observed from different view angles [180]. A statistical study based on *STEREO* observations indicated that at least about half of EUV jets exhibited a helical magnetic field structure [61]. Using the *SDO* data, Shen et al. [2] studied a rotating polar coronal hole jet which exhibited distinct bright helical structures around the jet axis; the authors proposed that the rotating jet was driven by the releasing of the magnetic twist stored in the pre-existing arch into the ambient open field through magnetic reconnection. Measurement results indicated that the period of rotation and the twists transferred into the open fields are about 564 seconds and 1.17–2.55 turns, respectively. Specifically, the statistical studies made by Moore et al. [64,186] found the existence of obvious axial rotation in both standard and blowout jets; their results showed that the number of turns of axial rotation ranges from 0.25 to 2.5. Other case studies showed that the number of turns of axial rotation ranges from about 0.34 to 4.7 [187–190], and the periods were measured to be 1–20 minutes [174,191,192].

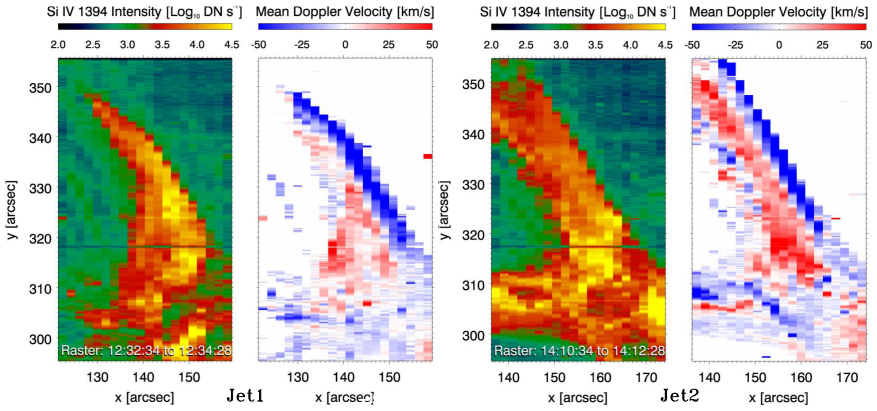

Figure 5. Spectroscopic observation of two rotating jets [194]. For each jet, total intensity and mean Doppler velocity are computed from *IRIS* Si IV 1394 line. In the doppler velocity maps, blue- and redshift signals are prominent around the northern and south edges of the jets.

The rotating motion of solar jets manifests as simultaneous blue- and redshift on the either side of the jet body in doppler velocity maps [88,108,181–183,193]. Pike & Mason [182] reported the appearance of simultaneous blue- and red-shifted emission on either side of macrospicules, which was interpreted as the presence of rotation plasma flows. Kamio et al. [183] reported similar doppler velocity patterns and measured that the blue- and redshift are about -120 and 50 km s^{-1}, respectively. Cheung et al. [194] studied four homologous helical jets at transition region temperatures, which showed evidence of oppositely directed flows with components reaching doppler velocities of $\pm$100 km s^{-1}, and the magnetic twist needed for the helical jets were found to be supplied by emerging current-carrying magnetic fields (see Figure 5). Lu et al. [195] studied a recurrent jet event using spectroscopic and stereoscopic observations, in which the doppler velocities were about $\pm$90 km s^{-1}, consistent with the value derived from stereoscopic imaging observations. Recent statistical study performed by Kayshap et al. [196] indicated that rotational motion is omnipresent in network jets, which can be detected as blueshift on one edge and redshift on the other at a mean rotational velocity of about 49.56 km s^{-1}.

(iii) Transverse Motion

Lateral expansion is a typical characteristic of solar jets, which manifests the whiplike upward motion of the newly formed field lines [88,129]. The typical expansion speeds was found to be tens of km s^{-1} [106,158,177]. Savcheva et al. [158] found that most X-ray jets exhibited lateral motions, which show some acceleration and deceleration before and after a period of constant lateral motion. Shimojo et al. [197] reported the successive slow (10 km s^{-1}) and fast (20 km s^{-1}) lateral expansions in an X-ray jet, in which the slow expanding stage was explained as the loop escaping from the anti-parallel magnetic field, while the fast stage was corresponding to the whiplike motion of the reconnected field lines. In contrast, Chandrashekhar et al. [198] proposed that the progressively reconnection occurring in magnetic structures along the neutral line could account for the slow lateral expansion motion of solar jets. Similar slow (16 km s^{-1}) and fast (135 km s^{-1}) expanding motions of loop systems were also observed in small chromospheric anemone jets [191], in which the transition from slow to fast expansion stage occurred at the start of the accompanying flares.

Shen et al. [2] reported an EUV jet in which the lateral expansion showed three distinct stages: slow (10 km s^{-1}), fast (25 km s^{-1}), and constant stages. Both the slow and fast expansion stages lasted for about 12 minutes, and the jet kept a constant width of about 4×10^4 km during the constant stage (left panels in Figure 6). The fast transition from the slow to the fast expansion stage

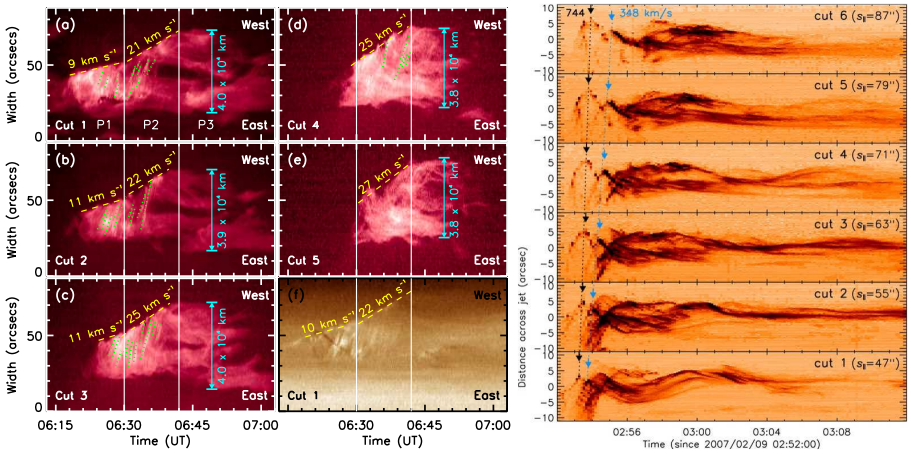

Figure 6. Examples of lateral expansion [2] (left) and transverse oscillation [199] (right) of solar jets, showing with time-distance plots perpendicular to the main axis of the jets at different heights. (a)–(e) and (f) are made from the *SDO* 304 Å and 193 Å observations, respectively. The expanding speeds and final width of the jet are indicated. The right panels are made from the *Hinode* Ca II H images. The black and blue arrows point to the crests of the first two inverted-V-shaped tracks. The dotted lines are linear fits to the propagation of the two crests, and the derived phase speeds are marked.

was explained as the sudden acceleration of the magnetic reconnection between the emerging arch and the ambient open field. In other words, the slow expansion stage corresponded to the emerging period of the arch, during which its reconnection with the ambient open field was slowly, while the fast expansion stage manifested the impulsive reconnection between the two magnetic systems. The constant stage indicated the fully opening of the closed arch and the end of the twist transfer into the open fields, and its width corresponds to the distance between the footpoints of the open field line and the remote footpoint of the closed arch. In a statistical study [64], the authors found that all blowout jets showed obvious lateral expansions but none in standard jets; the lack of lateral expansion in standard jets was possibly due to the smaller lateral plasma pressure in the jets than the magnetic pressure of the surrounding open field lines.

Transverse oscillation is another distinct characteristic of solar jets (right panels of Figure 6). Cirtain et al. [7] proposed that the transverse oscillation manifests the formation of Alfvén wave during the relaxation of the reconnected magnetic fields. Using the magneto seismology technique, the transverse oscillation of solar jets were used to derive some important physical parameters. For example, considering the transverse oscillation as kink mode oscillation [200], Morton et al. [201] estimated the temperature of a dark thread in a jet to be $2-3\times10^4$ K, therefore, the authors proposed that the dark thread was likely to have originated in the chromosphere. Using the measured wave parameters of a on-disk coronal hole jet and the magneto-seismological inversion technique, Chandrashekhar et al. [202] estimated the magnetic field strength along the jet spire to be about 1.2 Gauss. The speed and period of the transverse oscillations were measured to be, respectively, about 100-800 km s^{-1} and 200–536 seconds [7,191,199,201–203], consistent with theoretical prediction results of Alfvén waves in solar jets [7,88].

3. Relation to Other Phenomena

(a) Plume

Coronal plumes are thin ray-like structures pervasively within polar and equatorial coronal holes, as well as quiet-Sun regions [204–206]; they root in chromospheric networks and can be identified

over distances of several solar radii, and even in the interplanetary space. Solar jets show some common properties with plumes, for example, both are collimated magnetic structures resulting from magnetic reconnection between closed and open field lines [207,208].

Lites et al. [209] observed an EUV jet that embedded in a polar plume and caused notable density fluctuations within the plume structure. Ubiquitous episodic jets rooted in magnetized regions of the quiet corona were detected in plumes and interplume regions [205]. Raouafi et al. [210] studied 28 jets during the deep solar minimum and found that over 90% jets in their sample were associated with plumes, in which about 70% were followed by the formation of plumes with a time delay of minutes to hours, while the remaining jets occurred in pre-existing plumes and caused the brightness enhancement of the latter. Therefore, the authors proposed that solar jets are precursors of plumes. In addition, short-lived, jet-like events and transient bright points were identified at different locations within the base of preexisting long-lived plumes, which was thought to be important for the maintenance and change of the plume brightness. Raouafi & Stenborg [211] further found a large number of short-lived small jets and transient bright points caused by quasi-random cancellations between minority magnetic polarity with the ambient dominant open magnetic fields, confirming their previous finding that plumes are dependent on the occurrence of transients resulting from low-rate magnetic reconnection. However, solar jets may not be a necessary step for the formation and maintenance of plumes, because not all jets are accompanied by the formation of plumes, and the birth of plumes is sort of a follow up of the jet occurrence. Therefore, the relationship between jets and plumes needs further in-depth investigations.

(b) Filament

Solar jets are tightly associated with filaments. On the one hand, as what has been discussed in Section 2(b) and (c) (i), many solar jets are result from mini-filament eruptions, and the erupting filament material forms their cool component. On the other hand, solar jets can cause the oscillation, formation, and eruption of large-scale filaments [212–215].

Luna et al. [214] reported a case of large-amplitude longitudinal oscillation in a filament that was triggered by episodic jets along the filament axis; they proposed that the restoring force of the large-amplitude longitudinal filament oscillations was solar gravity, while the damping mechanism was the ongoing accumulation of mass onto the oscillating filament threads [216]. A similar event was reported by Awasthi et al. [217], in which the damping of the longitudinal filament oscillation was explained with the continued mass accretion supplied by the associated jets. Zhang et al. [215] reported the simultaneous transverse and longitudinal oscillations in a quiescent filament triggered by a coronal jet. Simultaneous transverse and longitudinal oscillations in filaments can also be excited by EUV waves [218]; it was found that the angle between the incoming waves and the filament axis is important to trigger which kind of oscillations [218,219]. This thought can be used to the generation of simultaneous transverse and longitudinal filament oscillations caused by jets. If a jet interacts with a filament along (perpendicular) to the filament axis, large-amplitude longitudinal (transverse) oscillation can be expected; if the jet interacts the filament with an acute angle with respect to the filament axis, simultaneous longitudinal and transverse oscillations can be launched.

Solar jets not only supply sufficient mass for filament formation but also cause the instability and eruption of large-scale filaments. Zirin [212] reported the formation of a short-lived filament caused by a surge through filling a semi-stable magnetic trap. Liu et al. [213] reported several similar events and found that the newly formed filaments exhibited distinct helical structures, whose lifetimes and average lengths were more than 20 hours and 145 Mm, respectively (see Figure 7). The authors proposed two necessary conditions for new filament formation by jets, namely, an empty filament channel (or magnetic trap) and enough mass supplied by surges. Guo et al. [220] studied the formation and eruption of a large filament associated with a recurrent surge event; they confirmed that surge activities can efficiently supply enough mass for the filament formation, and continuous mass with momentum supplied by surges can result in the

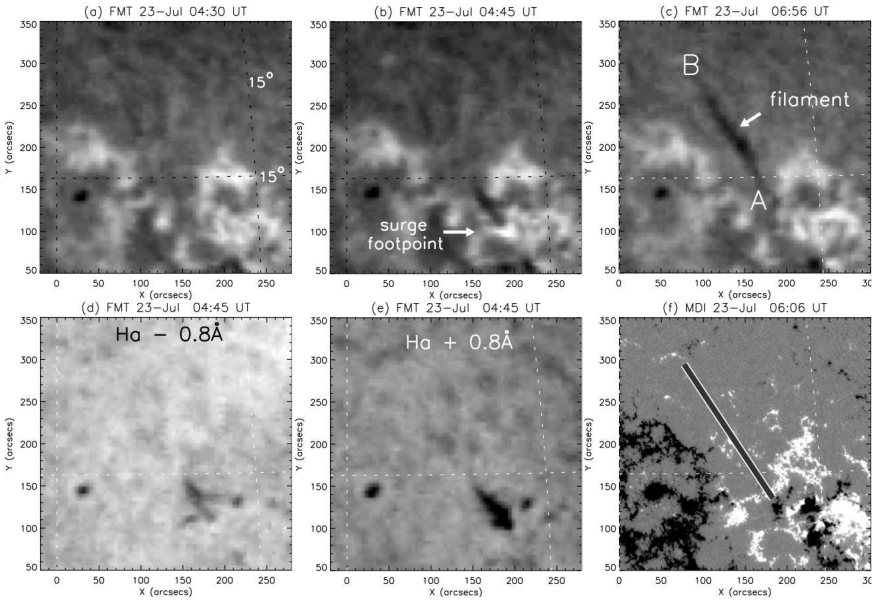

Figure 7. The formation of a filament due to the injection of jet material [213]. (a)–(c) are Hα-center images from the Flare Monitor Telescope; (d) and (e) are the blue- and red-wing images at ± 0.8 Å from the Hα center. The arrows in (b) and (c) indicate the surge and the newly formed filament, respectively. (f) is a *SOHO* magnetogram overlaid with the outline of the filament.

instability and even the eruption of the newly formed filament. Other similar studies suggest that the material for filament formation could be supplied by both of cool surges and hot coronal jets [221,222]. All the above studies showed that jet material was injected into filaments from one end of the filament channels. Recently, two-sided-loop jets in filament channels were found to be important the mass maintaining and eruption of large-scale filament. Shen et al. [43] reported that a two-sided-loop jet ejects material into an overlying large filament from below through magnetic reconnection, which provided an alternative way to understand how jet material injects into filament structures. In a recurrent two-sided-loop jet event occurred in a filament channel, Tian et al. [87] found that the first jet firstly caused the splitting of an overlying large filament into a double-decker filament, and then the following jets finally led to the fully eruption of the filament. These studies showed the close relationship between solar jets and filaments, but detailed physical connection between them still needs further observational and theoretical investigations.

(c) Magnetohydrodynamic Wave

Solar jets are closely related to MHD waves. Observational studies indicated that solar jets can act as a driver to excite torsion Alfvén waves in themselves (see Section 2 (d) (iii)), kink waves in remote coronal loops and filaments, and large-scale EUV waves. Statistical analysis indicated that the most probable mechanism for exciting kink oscillations of coronal loops is the deviation of loops from their equilibrium by nearby eruptions of plasma ejections [223,224]. Using the magneto seismology technique, the measured oscillation parameters could be used to derive the magnetic field strength of the loops/filaments. For example, Sarkar et al. [225] reported a case of jet-driven transverse oscillation of a coronal loop whose magnetic field strength was estimated to be about 2.68–4.5 Gauss. Luna et al. [214] estimated the minimum magnetic field strength of an oscillating filament to be about 14 Gauss. Zhang et al. [215] derived the curvature radius of the long arcade supporting the filament to be about 244 Mm.

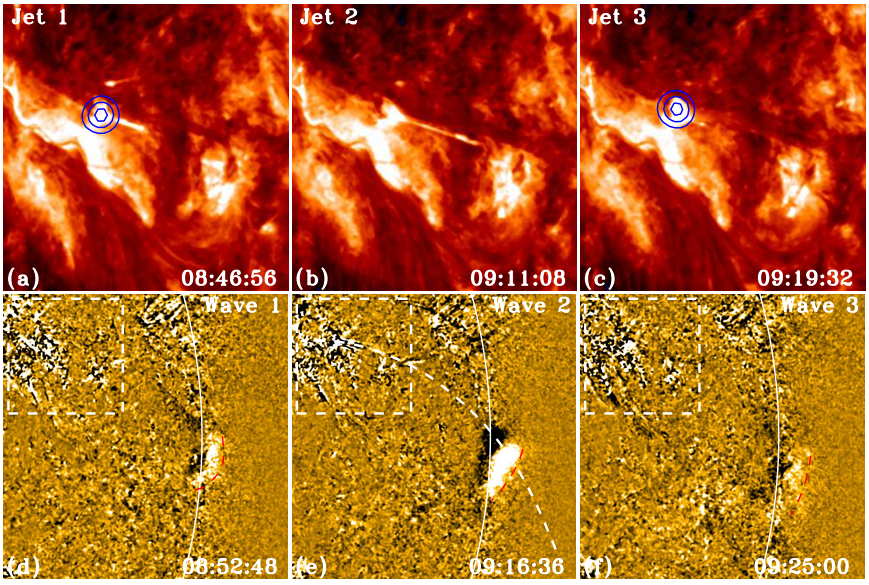

Figure 8. EUV waves driven by recurrent jets [94]. The top row shows three recurrent jets with the *SDO* 304 Å images, while the bottom row displays the corresponding EUV waves with the *SDO* 171 Å running difference images. The white boxes in the 171 Å images indicate the field-of-view of the 304 Å images. The blue contours in panels (a) and (c) indicate the *RHESSI* hard X-ray (HXR) sources, while the dashed red curves in the 171 Å images indicate the EUV waves.

Although many previous studies showed that large-scale EUV waves are driven by CMEs [226–230], recent observations suggest that they can also be launched by solar jets directly or indirectly. Shen et al. [231] reported that large-scale non-CME-association EUV waves were excited by the sudden lateral expansion of transequatorial loops due to the impingement of solar jets, in which the generation of the waves were caused by the sudden increase of gas and magnetic pressures around the expansion section of the loop. In a subsequent study, they further reported the generation of recurrent fast-mode EUV waves ahead of homologous jets along a large-scale transequatorial loop system (see Figure 8); they explained that the excitation mechanism of these waves resemble the generation mechanism of a piston shock in a tube [94]. Li et al. [232] also reported a nonlinear shock wave in a closed loop system driven by a coronal jet at one of the footpoint of the loop, the authors proposed that such kink of wave can quickly heat the corona plasma through the rarefaction wave. Simultaneous EUV wave, quasi-periodic fast-propagating wave, and kink waves were found to be launched during the interaction of a jet upon a coronal loop [224]. In addition, the expansion of the strongly curved reconnected loops in solar jets can also launch large-scale EUV waves [233]. A typical characteristic of these non-CME-association EUV waves is that their lifetimes (a few minutes) are much shorter than those driven by CMEs [231]. This is possibly because of that transient solar jets can not provide continuous driving to EUV waves like those driven by CMEs. EUV waves were evidenced to be important to trigger sympathetic solar activities, it was observed that coronal hole jets could be launched due to the passing of EUV waves [234]. This suggests that solar jets can also be produced by external disturbances except for internal magnetic activities such as flux cancellations and mini-filament eruptions.

(d) Coronal Mass Ejection

CMEs represent large-scale plasma and magnetic field releasing from the Sun into the interplanetary space [235–237]. CMEs with apparent angular width of 15° or less are typically

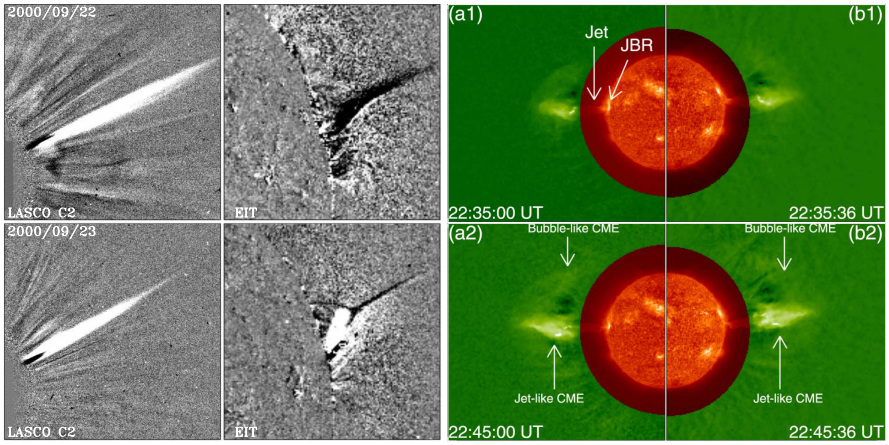

Figure 9. Left two columns: *SOHO* LASCO/C2 and 195 Å difference images show two narrow white-light jets in the coronagraph and on the disk limb [165]. Right two columns: *STEREO* 304 Å and the inner coronagraph difference images show a pair of simultaneous narrow and broad CMEs from two different view angles [240]. The bright feature in the source region and the jet are indicated by the arrows in (a1), while the narrow jet-like CME and the broad bubble-like CME are indicated by the arrows in (a2) and (b2), respectively.

associated with solar jets [238]. Observations suggested that solar jets can not only cause narrow jet-like CMEs [164] (see the left panels in Figure 9), but also standard broad CMEs with a typical three-part structure [239]. Sometimes, a paired narrow and board CMEs can be simultaneously launched by a single blowout jet [62,240] (see the right panels in Figure 9).

Narrow jet-like CMEs are simply the outward extensions of solar jets in the outer corona [94,164]. Statistical studies showed that during solar activity minimum the leading edges of jet-like CMEs propagate at speeds of 400-1100 km s^{-1}, while the bulk of their material travels at an average speeds of about 250 km s^{-1} at heliocentric distances of $2.9 - 3.7\,R_\odot$ [164]. In contrast, narrow jet-like CMEs during solar activity maximum have a typical speed of about 600 km s^{-1}, and they tend to be brighter and wider than those in solar activity minimum [165]. The propagation of jet-like CMEs did not regulated by the gravity along, since some of them exhibit accelerations rather than decelerations above $3\,R_\odot$ [241]. In addition, the direction of CMEs originated from solar jets can be significantly changed through interacting with other magnetic structures [242,243]. The on-disk progenitors of jet-like CMEs include flux emergence [244–246] and the eruption of mini-filaments [75,84,96,247,248]. Recently, Panesar et al. [249] studied many jets at the edge of an active region; they found that six of the homologous jets resulted in the so-called streamer-puff CMEs, and the CME-producing jets tended to be faster and longer-lasting than the non-CME-producing jets. Their observations also indicated that streamer-puff CMEs are due to the blowout of twisted streamer-base loops through magnetic reconnection.

Broad bubble-like CMEs with a typical three-part structure but on much smaller scales were found to be caused by solar jets [61], which are not simply the extension of jets into the outer corona, and their generation mechanism is possibly similar to large-scale CMEs. Jiang et al. [250] reported that sympathetic bubble-like CMEs can be launched through the impingement of a jet on remote interconnecting loops. Hong et al. [247] reported a micro-CME caused by a blowout jet that exhibited many observational characteristics as those identified in large-scale CMEs, suggesting the similarity between jet-driven micro-CMEs and large-scale CMEs [37]. Liu et al. [239] observed a jet-associated bubble-like CME whose bright core was evolved from the jet. Solar jets in or around active regions in association with fan-spine magnetic systems are often confined [55]. However, a few studies found that some broad CMEs are evolved from fan-spine eruptions [251]. For example, Li et al. [252] observed a broad CME that was caused by the eruption of a complicated fan-spine system in which a large fan-spine system hosted a small one below its fan.

The event started from the eruption of a mini-filament underneath the fan of the small fan-spine system, which firstly triggered the nullpoint reconnection within the small fan-spine system; then the eruption of the small fan-spine system further triggered the nullpoint reconnection within the large fan-spine system. Here, the successful formation of CMEs from fan-spine eruptions might be due to the weak magnetic confinement of the overlying magnetic fields or sufficient energy released during the associated flares [236].

Shen et al. [62] reported an interesting event in which a pair of narrow and broad CMEs were dynamically connected to a single blowout jet which showed cool and hot components. Similar event was possibly observed by Ko et al. [116], where they detected both cool and hot components in a jet and the appearance of both jet-like and bubble-like CME pair in the coronagraph. However, due to the low resolution observations they used, the authors did not establish the physical relation between the CMEs and the jet. Shen et al. [62] proposed a cartoon model to interpret the generation of the cool and hot components and the formation of the paired CMEs. According to their interpretation, the hot component is the outward moving heated plasma flow generated and accelerated by the external reconnection between the base arch and the ambient open field lines, and it further evolves into the narrow jet-like CME in the outer corona. In the meantime, the external reconnection removes the confining fields of the mini-filament, which therefore leads to the rising of the mini-filament and the formation of an internal current sheet between the two legs of the confining field lines. Finally, the reconnection in the internal current sheet further results in the full eruption of the mini-filament and the formation of the broad bubble-like CME, during which the erupting filament material forms the jet's cool component. Recently, more and more observations evidenced the appearance of paired narrow and broad CMEs in association with on-disk blowout jets [155,240,243,253,254], and the phenomenological model of Shen et al. [62] provides a possible explanation for these observations but further observational and numerical investigation is required to confirm this scenario.

(e) Particle Acceleration

Solar energetic particles (SEP) carry important information about the particle energization inside the solar corona, as well as the properties of the acceleration volume. SEP events are divided into "gradual" and "impulsive" types. Gradual SEP events are long-lasting, intense, more closely correlated with CMEs, and characterized by the abundances and charge states of the solar wind. Therefore, they are thought to be accelerated by CME-driven coronal/interplanetary shock waves. In contrast, impulsive SEP events are short lived, less intense, closely related to flaring active regions, characterized by high $^3\mathrm{He}/^4\mathrm{He}$ ratios and high ionization states, and tightly correlated with type III radio bursts [255].

Flaring regions accompanied by solar jets are found to be the most possible candidate solar source for producing impulsive SEP events [256], since the magnetic field along which a jet emerges is open to interplanetary space, offering a clear "escape route" for flare accelerated particles. In radio observations, type III bursts are produced by electrons streaming along open field lines extending to interplanetary space. Many studies indicated that type III radio bursts and SEP events are spatially and temporally associated with solar jets [69,257–262]. Wang et al. [263] investigated 25 ^{3}He-rich events and found that their sources lie close to coronal holes and characterized by jet-like ejections along Earth-directed open field lines. Some studies suggested that impulsive SEP events are associated with narrow jet-like CMEs [263–266]. Nitta et al. [267] found that the solar source regions of SEP events are often accompanied by solar jets preceded by type III radio bursts, and about 80% events showed open field lines in or around their source regions. In addition, ^{3}He-rich SEPs were also observed to be associated with helical jets [268,268], and the solar source regions could be small active regions near coronal holes [263,266,268], plage regions [269], and sunspots [270,271].

Type III radio burst is an important diagnostic tool for SEPs. It is a signature of propagating nonthermal electron beams in a wide range of heights of the solar atmosphere (from the low corona to the interplanetary space), and is excited at the fundamental and second harmonic of

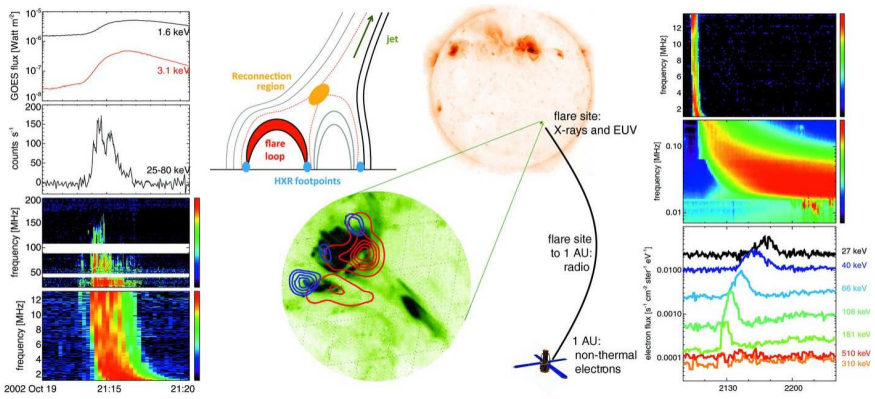

Figure 10. Schematic describing prompt SEP events [273]. Time series data track energetic electrons from the Sun into interplanetary space are plotted on the left and right, including soft and HXRs, radio waves, and non-thermal electrons seen near 1 AU. The center shows the results of HXR and EUV observations and a schematic of jet model. The reconnection region, the flare loop, the HXR footpoints, and the jet are labeled.

the local electron plasma frequency ($f_{pe} \approx 9\sqrt{n_e}$ kHz, here n_e is the electro number density) by the Langmuir waves generated by the electron beam instabilities [272]. Since the electron number density of the corona decreases rapidly with the increasing height, a type III radio burst drifts from high (low) to low (high) frequencies reflecting the upward (downward) moving electron beams. Chen et al. [260,262] derived the trajectories of electron beams in the low corona and found that each group of electron beams diverges from an extremely compact region that located behind the erupting jet spire but above the closed arcades, coinciding with the location of magnetic reconnection predicted in jet models.

Type III radio burst is an excellent qualitative maker of accelerated electrons and their paths, but it can not be used to quantitatively measure the emitting electron distributions due to the nonlinear processes in its generation [272]. A complementary diagnostic tool for studying accelerated electron distributions is HXR observation, which is dominated by footpoint emission in the dense chromosphere due to the downward propagating electron beams, but emission from escaping electron beams in the low density corona is typically too faint to be observed [274]. Glesener et al. [275] analyzed the accelerated electron distributions in a jet-associated event using simultaneous HXR and microwave data and found that the HXR time profile above 20 KeV matches that of the accompanying type III and broadband gyrosynchrotron radio emission, indicating both accelerated electrons escaping outward along the jet path and those trapped in the flare loop. Using combined radio and HXR observations, Krucker et al. [273] observationally confirmed the three expectant HXR sources in solar jets as those predicted in jet models, in which two sources are at the footpoints of the post-flare loop, and the other one is at the footpoint of the newly formed opened field lines (see Figure 10).

Above studies highly suggested that impulsive SEP events are tightly associated with solar jets, and they are mostly accelerated by the mechanism of interchange reconnection. However, the detailed acceleration mechanism of SEPs is still an unresolved question, although several possible theoretical mechanisms have been proposed to account for the acceleration of SEPs [276–278].

(f) Coronal Heating and Solar Wind

The problems of coronal heating and the acceleration of solar wind are two highly controversial topics in solar physics. Since energy must come from the solar interior, it is hard to understand why coronal temperature is extremely hotter than the solar surface. The problem is primarily concerned with how energy is continuously transported up into the corona through nonthermal

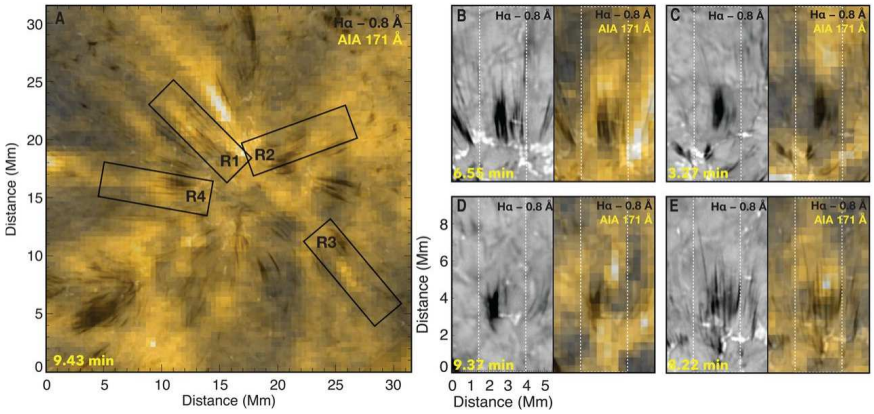

Figure 11. Heating effect caused by spicular activities [9]. The left panel shows a *SDO* 171 Å image (yellow) overlaid with the Hα blue wing image (grayscale) from GST. The Hα blue wing and the same image overlain with the *SDO* 171 Å image are shown in each pair of panels on the right, in which the white dotted boxes correspond to the box regions (R1–R4) in the left panel.

processes from the solar interior and then convert it into heat within a few solar radii. In the last half-century, many coronal heating theories have been proposed, but two theories have remained as the most likely candidates: wave heating and magnetic reconnection [279]. Solar wind is composed of charged particles including neutral atoms, positive charged ions, and free electrons, which is released from the upper solar atmosphere and fill the majority of the volume of the solar system. Solar wind has two fundamental states: slow and fast solar winds. While their compositions and temperatures are similar to the corona, their average velocities in near-Earth space are respectively about 300–500 km s^{-1} and 750 km s^{-1} for slow and fast solar winds [280]. Previous studies suggested that the slow solar wind appears to originate from a region around the Sun's equatorial belt that is known as the streamer belt, while coronal holes that consist of funnel-like regions of open field lines are regarded as the solar source of the fast solar wind. However, the detailed origin and acceleration of solar wind is still not understood and cannot be fully explained by current theory [281]. Recent observations suggested that high frequency but small-scale solar jets (also called spicules, fibrils, and microjets) seems significant important for supplying mass and energy to power the corona and the solar wind [282].

Ultraviolet spectrum observations revealed prevalent high-energy jets in the corona at an average speed of 400 km s^{-1}, whose energy and mass can satisfy the power (6×10^{27} erg s^{-1}) and mass flux (2×10^{12} g s^{-1}) requirements of the corona and solar wind if one assume a birthrate of 24 events per second over the whole Sun [6]. Shibata et al. [1] proposed that chromospheric jets, which have a width (length) of 0.15–0.3 (2–5) Mm and eject at a speed of 10–20 km s^{-1}, may play an important role in heating coronal plasma as the nanoflare scenario [283]. The one-to-one relation between chromospheric jets and their coronal counterparts were examined in detail [284], which showed that chromospheric plasma was propelled upward with speeds of about 50–100 km s^{-1}, and with the bulk of the mass rapidly heated to transition region temperature. A little bit later, plasma directly associated with these jets was heated to coronal temperature of at least 1–2 MK, at the bottom during the initial states, and both along and toward the top of the chromospheric feature. Very recently, Samanta et al. [9] found that enhanced coronal emission generally appeared at the top of chromospheric spicular jets, which implied that the chromospheric spicular jets channelled hot plasma into the corona, and it provided a link between magnetic activities in the lower atmosphere and coronal heating (see Figure 11). In addition, solar jets also excite shocks ahead of them and drive KH instability at their boundaries; the dissipation of shocks and reconnection within the vortex structures also release energy to heat the corona [6,94,153].

Alfvén waves, which propagate along magnetic field lines over large distances and transport magnetoconvective energy from near the photosphere into the corona, have been invoked as a possible candidate to heat coronal plasma to millions of degrees and to accelerate the solar wind to hundreds of km s^{-1}. Transverse oscillations of spicular jets were regarded as the presence or passage of Alfvén waves; the energy carried by these Alfvén waves was found to be enough to accelerate solar wind and to heat the quiet corona [285–288]. Cirtain et al. [7] detected two distinct speeds of solar X-ray jets, in which one is near the Alfvén speed ($\sim$800 km s^{-1}) and the other near the sound speed ($\sim$200 km s^{-1}). The authors claimed that a large number of X-ray jets with high velocities may contribute to high-speed solar wind. McIntosh et al. [289] found that a significant portion of the energy responsible for the transport of heated mass into the fast solar wind was provided by episodically occurring small-scale jets in the upper chromosphere and transition region. Tian et al. [290] found two types of doppler shift oscillations in the corona, in which one was at the loop footpoint regions with a dominant period around 10 minutes, while the other was associated with the upper part of loops with a period of 3–6 minutes. The authors argued that the first type is quasi-periodic upflows associated with small-scale jets and it plays an important role in the supply of mass and energy to the hot corona, while the second type is kink/Alfvén waves (see also De Moortel et al. [291] and Threlfall et al. [292]). Recent *IRIS* observations also reveled the prevalence of small-scale jets from the networks of solar transition region and chromosphere [8]; they originate from small-scale bright regions and preceded by footpoint brightenings, ejecting at a speed of 80–250 km s^{-1} and are accompanied by transverse waves with amplitudes of about 20 km s^{-1}. They were thought to be an intermittent but persistent source of mass and energy for solar wind.

For big jets that often reach up to a few solar radii and can be observed as white-light jets or jet-like CMEs; their contribution to solar wind often exhibit as microstreams or speed enhancements [211,293–295]. It was found that these jets are not sufficient to explain the fast solar wind [296]. Observations indicated that the motions of white-light jets are not consistent with the ballistic behavior, and some of them even exhibit slight accelerations instead of decelerations above 3 $R_{\odot}$. This suggested that the motions of white-light jets are regulated by other forces besides the gravity. In addition, the bulk of almost all white-light jets travel at lower velocities averaging around 250 km s^{-1} at heliocentric distances of a few solar radii. These observational facts may imply that the moving jets have been incorporated into the ambient solar wind [164,241]. Yu et al. [297] found that fast solar polar jets show a positive correlation with high-speed responses traced into the interplanetary medium, and they contributed about 3.2% (1.6%) of the mass (energy) of solar wind. The authors further analyzed the responses in the solar wind resulting from a high-speed jet at a speed of about 1200 km s^{-1}; they found an ubiquitous presence in polar coronal regions at about 100-fold mass and energy greater than the coronal response itself. This suggests that the primary acceleration of solar wind should induce the dissipation of high-speed solar jets [298].

4. Physical Interpretation and Modeling

With the unceasing improvement of solar telescopes and numerical modeling, the physical interpretation of solar jets have achieved significant progresses in recent years. In theoretical studies, the mechanism of flux emergence and onset of instability or loss of equilibrium were investigated in detail, in which the slingshot effect, untwisting, and chromospheric evaporation were considered as the possible acceleration mechanisms [33]. As more and more observational studies revealed that solar jets are caused by the eruption of mini-filaments in association with flux cancellations, new models were also developed to account for these new features. Although there are various aspects that have not yet been fully addressed, the results of the current simulations have been in reasonably good agreement with the observations including morphology, velocities, and basic plasma properties.

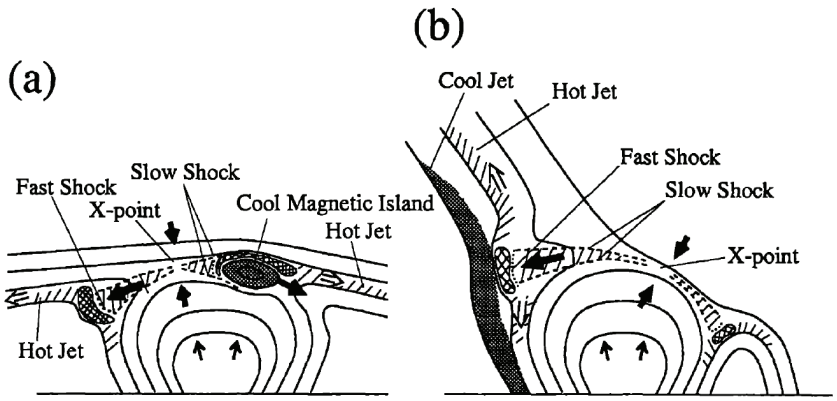

Figure 12. Schematic diagrams for the numerical models of two-sided-loop jets (left) and anemone jets (right), in which the arrows show the moving direction of the magnetic field lines, and features including the X-point, slow and fast shocks, cool and hot jets are indicated [140].

(a) Emerging-Reconnection Model

Heyvaerts et al. [299] proposed an emerging-reconnection model for explaining solar flares and surges. This mechanism was also proposed for the onset of CMEs [300]. Shibata et al. [106] found that many X-ray jets are associated with emerging flux regions, and started with formation and ejection of magnetic plasmoids; they therefore proposed that the emerging-reconnection scenario could be a possible explanation for solar jets. This scenario was tested with 2D MHD simulation without considering the effect of heat conduction and radiative cooling [129,140], which showed that simultaneous hot X-ray jet and cool Hα surge are generated by magnetic reconnection between emerging fluxes and ambient pre-existing magnetic fields (see Figure 12). The hot jet is the secondary jet accelerated by the enhanced thermal pressure gradient behind the fast shock caused by the collision of the reconnection outflow with the ambient magnetic field, while the cool surge is formed by the cold chromospheric plasma that is carried up by the emerging flux and accelerated by the tension force of the reconnected field lines (slingshot effect). The reconnection outflow from the current sheet is composed of many plasmoids produced by tearing and coalescence instabilities, which represent miniature flux ropes in 3D [106,144–146]. The emerging-reconnection scenario was intensively studied in previous articles with 2D and 3D simulations by considering more realistic physical condition, and the results could be applied to explain many characteristics of solar jets (see [33,145,301–303] for details).

Although there are many theoretical studies of the emerging-reconnection scenario in the literature, the explicit observational evidence for flux emergence directly driving jets is so far limited. In an emerging active region, Li et al. [163] observed 575 jets, in which most of them occurred at the periphery region of the emerging fluxes. However, the authors did not figure out the relationship between the jets and the flux emergence. In many observations, opposite polarities firstly show emergence and then followed by flux cancellation, and the associated jets often occurred right after the start of flux cancellation [37,46,62,69,87]. Such a magnetic flux variation pattern often suggest the triggering of the jets should be flux cancellations. One possible example of this case was presented by Cheung et al. [194]; however, since the jet eruption source region was very dynamic with mixed polarity, it hard to say if the jet was directly caused by flux emergence or not. Panesar et al. [98] augured that the reason for flux emergence not directly causing jets is because the speed of emergence is seldom, if ever, fast enough. The emerging-reconnection scenario was challenged by the discovery of blowout jets that often involve the eruption of mini-filaments or filament-channels [36,62,63,69,97] in association with flux cancellations [43,66,68,247,304–308], and the cool component of blowout jets is actually

the erupting filament material itself [43,62,69] rather than chromospheric material carrying up by emerging flux and accelerated by magnetic tension force as proposed in the emerging-reconnection model [129]. In a statistical study of 27 equatorial coronal hole jets, Kumar et al. [97] found six jets (22%) were apparently associated with flux cancellations, while the remaining events did not show measurable flux emergence or cancellation associated with the eruption. Therefore, the ultimate trigger source of solar jets still requires further investigation. One should keep in mind that the emergence aspects of the models introduced in following sub-sections is still subject to verification.

(b) Embedded-Bipole Model

Pariat et al. [309] proposed the embedded-dipole model to interpret rotating solar jets. The model adopted an axisymmetrical fan-spine topology that hosts a nullpoint within the system, in which magnetic free energy is injected slowly by footpoint motions that introduce twist within the closed dome, and is released rapidly by the onset of an ideal kink instability. Since reconnection is forbidden for the axisymmetrical nullpoint topology, explosive energy release via reconnection can only occur when the symmetry of the system is broken by the occurring of kink instability until the magnetic stress builds up to a high level. The reconnection between the twisted, close and the ambient untwisted, open field lines launches a torsional Alfvén wave which compresses and accelerates the plasma along the reconnected open field lines upwardly. Eventually, an upward ejecting helical rotating jet is generated, and it has similar geometrical features as observations, such as the inverted-Y shape, the drift of the jet axis [106], helical structure [2,62,180], and Alfvén waves within jets [7,199]. It was found that this mechanism can efficiently release about 90% free energy stored in the embedded bipole topology. If a stress is constantly applied at the photospheric boundary, recurrent rotating jets can be launched [310]. In such a symmetric configuration, Rachmeler et al. [311] found that reconnection is fundamental for jet formation. Recently, the embedded-bipole model was subsequently extended for studying the influence of magnetic field geometry [312], plasma beta [313], gravity [314], and the characteristic lengths of the spine and fan structures [315]. In addition, the possible applications of the embedded-dipole model to interpret standard and blowout jets [312], the formation of plasmoids [146], and microstreams and torsional Alfvén waves in the solar wind [314] were also explored in great detail.

(c) Breakout Jet Model

The magnetic breakout model was originally proposed to interpret the initiation of large-scale CMEs, in which magnetic reconnection between the unsheared field and neighboring flux systems decreases the amount of the overlying field and, thereby, allows the low-lying sheared flux to breakout [316]. So far, the magnetic breakout model has been confirmed by many observational studies [237,317].

Recently, high-resolution observational and statistical studies suggested that all coronal jets are probably driven by mini-filament eruptions, and they share many common characteristics with large-scale eruptions. Therefore, coronal jets are proposed to be the miniature version of large-scale eruptions [33,36,62–64,74,186,247]. In this line of thought, Wyper et al. [318] performed an ultrahigh-resolution 3D MHD simulation to test this hypothesis, using the above mentioned embedded-dipole scenario (see Figure 13). The initial magnetic configuration is a fan-spine structure, which is current-free and therefore has no filament and no free energy within it to power an eruption. Through shearing the footpoints of field lines connecting to the parasitic polarity over a finite time interval, the system is energized and a twisted filament structure is generated underneath the fan structure. The confining field lines of the filament expands upward towards the nullpoint and creates a current sheet between the confining field and the ambient open field. The (external) reconnection in this current sheet removes the confining field of the filament, allowing the filament to rise. Subsequently, (internal) reconnection starts underneath

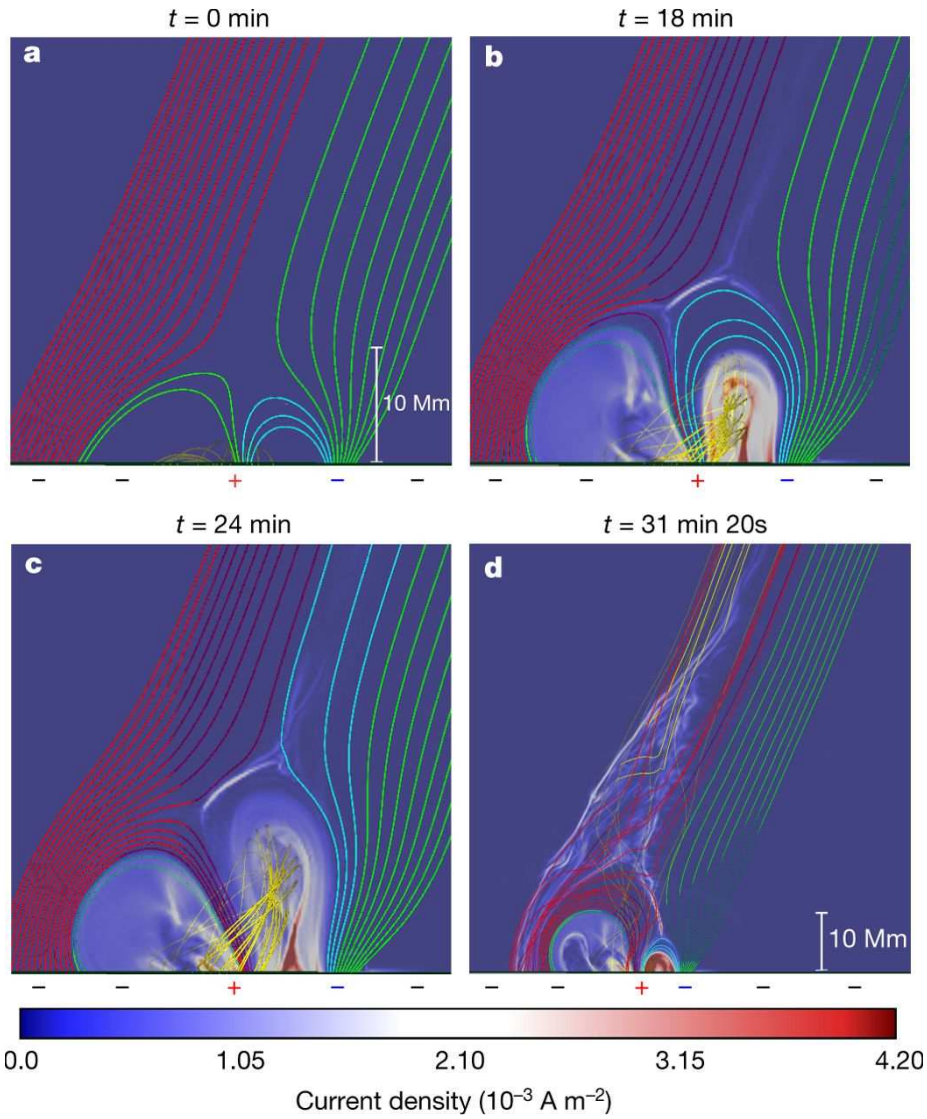

Figure 13. The evolution configuration of the breakout jet model [318]. Field lines with different colors represent different connectivity domains, and the positive and negative polarities are respectively indicated by the plus and minus symbols. The yellow curves depict the filament or flux rope formed beneath the central arcade. The current density is displayed as semi-transparent shading (color scale), and high current density regions can be identified as thin strips under beneath the filament (d) and the center of the simulation domain (b and c).

the filament possibly enhanced by the kink or torus instability, which eventually leads to the violent eruption of the system and the formation of a rotating jet along the reconnected open field lines. The simulated jet is accelerated by torsional Alfvén wave launched when the twist in the filament begins to transfer into the ambient open field through magnetic reconnection, and the jet body is composed of hot and cool plasma flows originated form the reconnection region and the filament, respectively. In this model, the eruption is due to reconnection rather than ideal instability as proposed in the embedded bipole model [309], and the physical process is similar to the magnetic breakout model. Therefore, the authors named their model as breakout jet model, and claimed that the magnetic breakout model is a universal model for solar eruptions

regardless of their scales. In subsequent studies, the authors further used their model to explain observational features of solar jets [319–321].

(d) Data-constrained and Data-driven models

To obtain realistic numerical results that are more comparable with real observations, some works managed to use multi-wavelength observations in tandem with MHD simulations to investigate the formation and evolution of solar jets. Such kind of simulations are known as data-driven models, which use continuously time-varying solar observations as input to reproduce solar jets. In contrast, if one use one instantaneous cadence of observation as input, it should be called data-constrained modeling.

Jiang et al. [322] simulated a jet-like eruption in a realistic and self-consistent way from its origin to onset with a data-driven MHD model; their result is well consistent with EUV observations. The authors found that the transition from the pre-eruptive to eruptive state is due to the magnetic reconnection between a stressed emerging and expanding arcade and the ambient pre-existing open field, in agreement with the physical picture described in anemone jet models [129,301]. In addition, their simulation also revealed that the non-potential magnetic flux emergence not only continuously injects magnetic free energy/helicity into the system due to photospheric shearing motions, but also stresses the field to form an intense current sheet.

Using extrapolated non-force-free magnetic field as the initial condition, Nayak et al. [323] performed a data-constrained MHD simulation to study blowout jets. In their simulation, the plasma is idealized to be incompressible, thermally homogeneous and having perfect electrical conductivity. They found that the initiation of the jet is due to the magnetic reconnection near a set of two 3D magnetic nullpoints, and the jet itself is evolved from a flux rope near the nullpoints through changing the flux rope's magnetic field lines from an anchored to an open topology. In addition, the generation of flare ribbons is found to be attributed to reconnections at a 3D nullpoint and a quasi-separatrix layer, consistent with previous data-constrained simulation of circular flares [50] and the observations of confined fan-spine jets [55].

Cheung et al. [194] presented the data-constrained simulations of four homologous helical jets originated from a fan-spine magnetic system. Based on the extrapolated potential magnetic field, the authors used the time-dependent magnetofrictional method [324] to carry out the numerical simulation of the coronal field evolution. Their result showed that the emergence of current-carrying magnetic field supplies the magnetic twist needed for the formation of recurrent helical jets. Since the magnetofrictional method calculates the evolution of the magnetic field through a series of quasi-static equilibria in response to photospheric footpoint motions, it can capture the response of the relax of a magnetic configuration to the Lorentz force, but it can not reveal the heating process of the cool plasma by the stored magnetic energy, as well as the acceleration mechanism of the ejecting plasma. Meyer et al. [325] presented eight different simulations to demonstrate the structure of coronal jets in unipolar regions, in which the coronal magnetic field is evolved in time using the magnetofrictional technique. The investigated photospheric magnetic field configurations include a single parasitic polarity rotating or moving in a circular path, opposite polarity pairs involved in flyby (shearing), cancellation, and emergence. Although the simulations can not model the dynamic eruptive stage of the jets, it can be used to diagnose the building of magnetic energy and the formation of the jet structures. The authors found that certain configurations and motions, such as twisting and shearing, can produce a twisted flux rope and allow the significant buildup of free energy, and they can be viewed as the progenitors of blowout jets; other simpler configurations are more comparable to the standard jets.

(e) Large-scale Interplanetary Jet

Most previous simulations were performed within a small numerical domains in Cartesian geometry to study the generation mechanism and evolution process. So far, only a few

publications considered a large simulation domain extension to the interplanetary space using spherical geometry to investigate the interplanetary effects caused by solar jets.

Török et al. [326] and Lionello et al. [327] performed a 3D, viscous, resistive MHD simulation in spherical coordinates. The simulation domain covers the corona from $1-20\,R_\odot$, and the effects of radiative losses, thermal conduction parallel to the magnetic field, and an empirical coronal heating function are all considered. The simulation adopted the flux emergence scenario to generate the jet in the low corona, in which the authors evidenced the transition of a standard jet to blowout jet if the emergence is imposed for a long time, resembling other 3D emerging-reconnection models [145]. A white-light CME is identified two hours after the launch of the standard jet. Several plasmoids are identified along the CME, which manifested the episodic reconnection outflows at larger heights. It was estimated that the total energy and mass provided by the jet to the background solar wind are about (0.3–1.0)% and (0.3–3.0)%, respectively. In addition, the authors found that blowout jets can produce a stronger perturbation in the solar wind than standard ones.

To investigate the influence of solar jets to the solar wind, Karpen et al. [314] extended the embedded bipole model [309] by including spherical geometry, gravity, and solar wind in a nonuniform, coronal hole-like ambient atmosphere. Similar to previous works, they launched a helical jet due to the resistive kink-like instability that drives fast reconnection across the closed-open separatrix; they found that the jet propagation is sustained through the outer corona, in the form of a traveling nonlinear Alfvén wave front trailed by slower-moving plasma density enhancements that are compressed and accelerated by the wave. The authors claimed that their results agree well with observations of white-light jets, and can explain microstreams and torsional Alfvén waves detected in situ in the solar wind. Using another code that employs Alfvén wave dissipation to produce a realistic solar wind background, Szente et al. [328] studied the effects of coronal jets on the global corona and their contribution to the solar wind. A reconnection-driven blowout jet similar to that described by Pariat et al. [309] is generated, and its physical structure, dynamics, and emission are close matching with the observed EUV and X-ray jets. The authors found that the large-scale corona is affected significantly by the outwardly propagating torsional Alfvén waves generated by the jet (across 40° in latitude and out to $24\,R_\odot$). The simulation also showed that the magnetic untwisting loses most of its energy in the low corona below $2.2\,R_\odot$, but the introduced magnetic perturbation can propagate out to $24\,R_\odot$ within 3 hours. Consistent with observational results [297,298], the above simulations confirmed the conjecture that coronal jets provide only a small amount of mass and energy to the solar wind.

5. Conclusion and Prospects

High spatiotemporal resolution imaging, spectroscopic, and stereoscopic observations covering a wide temperature range over the last several decades significantly improved our understanding of solar jets, including various aspects such as their triggering, formation, evolution, fine structure, relationships with other solar eruptive activities, and the possible contribution to the coronal heating and the acceleration of solar wind. Nowadays, we recognize that the basic energy release mechanism in solar jets is magnetic reconnection; they are triggered by photospheric magnetic activities exhibiting as flux flux cancellation and shearing motions of opposite polarities, and accelerated alone or in combination by possible mechanisms of untwisting, chromospheric evaporation, and slingshot effect. Observationally, solar jets can be divided into eruptive jets and confined jets, or straight anemone jets and two-sided-loop jets; they can evolve from different progenitors including satellite sunspots (or small opposite-polarity magnetic elements), mini-filaments, coronal bright points, and mini-sigmoids, exhibit various fine structures including cool and hot components, plasmoid, and KH vortex structures, and show interesting rotating and transverse oscillation motions. Solar jets not only provide necessary mass and energy to the corona and solar wind, trigger other eruptive phenomena such as EUV waves, filament and loop oscillations, and CMEs, but also significantly affect the interplanetary space through launching CMEs and energetic particles. One of the new knowledge we have gained in recent years is that

solar jets are often driven by mini-filament eruptions in association with photospheric magnetic flux cancellations; besides narrow white-light jets, broad CMEs with typical three-part structure and simultaneous paired narrow and broad CMEs are found to be dynamically associated with solar jets. These findings lead to an important conclusion that solar jets may represent the miniature version of large-scale solar eruptions, and it probably hints at a scale invariance of solar eruptions. In this sense, investigating solar jets can provide important clues to understand complicated large-scale solar eruptions (e.g., CMEs) and currently indistinguishable small-scale transients (e.g., spicules).

Numerical modeling of solar jets is also achieved many significant advances in recent years. MHD models of solar jets have been developed from 1D to 3D with different scenarios such as the emerging-reconnection and onset of instability mechanisms, which can be applied to interpret the formation, evolution, morphology, and plasma properties of standard and blowout jets in coronal holes and active regions. Recently, some numerical works further consider the effects of heat conduction, radiative losses, and background heating, and more realistic data-constrained and data-driven MHD simulations are being developed to understand solar jets. These great efforts make the obtained numerical results are more morphologically and quantificational comparable with real observations. In addition, numerical works by considering a large domain extension to the interplanetary space using spherical geometry are also developed for understanding the interplanetary disturbances resulted from solar jets.

Despite the great advances obtained in previous observational and numerical studies, there are still many aspects of solar jets deserve further investigations. The following is a list of some outstanding questions:

(i) Observations showed that solar jets are tightly associated with magnetic flux cancellation, especially in mini-filament-driven jets. Nevertheless, what kind of physical process undergoes during the triggering stage is still unclear. Physically, flux cancellation represents three possible processes: emergence of U-shaped loops, submergence of Ω-shaped loops, and reconnection in the magnetogram layer [329]. Therefore, which process and how flux cancellation trigger a solar jet need to be clarified in future observational and numerical works. In addition, although there are many models have been developed based on the emergence-reconnection scenario, explicit evidence for flux emergence directly driving jets is still very limited. Therefore, these models should be verified with more observational evidences.

(ii) Observational studies indicated that solar jets can not only cause narrow white-light jets in the outer corona, they can also result in broad CMEs with typical three-part structure. Sometimes, a single mini-filament-driven jet can cause a pair of simultaneous narrow and broad CMEs [62]. Narrow white-light jets are simply the extension of solar jets into the outer corona; however, the physical relationship between solar jets and broad and simultaneous paired narrow and broad CMEs are still unclear. Although the formation of solar jets in the low corona has been intensively studied with 3D MHD simulations, there still no theoretical or simulation works for understanding how can a straight, linear solar jet cause broad and paired narrow and broad CMEs in the outer corona. Therefore, this aspect deserves further observational and theoretical investigations, and this kind of study can also help us to understand the similarity between small- and large-scale solar eruptions.

(iii) Although more and more observational showed the similarity between small-scale solar jets and large-scale filament/CME eruptions, the possible scale invariance of solar eruptions should be further tested theoretically and observationally. It should be significative to check whether the current jet models can be applied to small-scale explosions such as spicules and nano-flares which are believed to be important for coronal heating. On the other hand, it is also important to check if the current jet models are suitable for explaining complicated large-scale solar eruptions and astrophysical jets.

(iv) The contribution of solar jets to coronal heating and the formation and acceleration of solar wind, and the jet-associated acceleration mechanism of solar energetic particles should be investigated in-depth. There are too much guessing and uncertainties in the existing studies on these topics.

(v) Most of the current MHD simulations only deal with idealized boundary and initial conditions using a relatively small numerical domain. Future investigations should consider more realistic data-constrained and data-driven MHD simulations, and using a large simulation domain so that one can study the interplanetary disturbances caused by solar jets.

The investigation of solar jets will benefit from future ground-based large-aperture solar telescopes and advanced space missions. For example, the *Parker Solar Probe* (*PSP* [330]) launched in 2018 will observe the Sun within $9.86\ R_\odot$ by 2025, which means that it will fly through coronal structures such as solar jets and CMEs, which can provide in suit detection of physical parameters. The *Solar Orbiter* [331] launched in 2020 will operate both in and out of the ecliptic plane, which will image the polar regions of the Sun where solar jets are prominent, and can provide an opportunity for stereoscopic diagnosing of solar jets in combination with other telescopes on geosynchronous orbit. The 4-meter ground-based Daniel K. Inouye Solar Telescope [332] under construction has obtained its first images which can distinguish solar features as small as 30 km in size. The ultrahigh spatial resolution observations will help us to resolve the triggering and formation problems of solar jets, as well as small spicules. The *Advanced Space-based Solar Observatory* (*ASO-S* [333]) that will be launched in 2021 will provided coronagraph, photospheric magnetic field, and hard X-ray observations for the investigation of solar jets. A combination measurements of magnetic field, spectroscopy, imaging, and in situ observations provided by above telescopes will undoubtedly make significant breakthrough in our understanding of the physics of solar jets and the related phenomena.

Data Accessibility. This article has no additional data.

Competing Interests. We declare we have no competing interests.

Funding. This work was supported by the Natural Science Foundation of China (11922307, 11773068, and 11633008), the Yunnan Science Foundation (2017FB006), and the West Light Foundation of Chinese Academy of Sciences.

Acknowledgements. The author thanks the referees who provide many valuable suggestions and comments for improving the quality of the present paper, and appreciate the helpful discussions with Dr. Y. Liu, L. Yang, J. Hong and their careful reading of the manuscript.

References

1. Shibata K, Nakamura T, Matsumoto T, Otsuji K, Okamoto TJ, Nishizuka N, Kawate T, Watanabe H, Nagata S, UeNo S, et al.. 2007 Chromospheric Anemone Jets as Evidence of Ubiquitous Reconnection. *Science* **318**, 1591.
2. Shen Y, Liu Y, Su J, Ibrahim A. 2011 Kinematics and Fine Structure of an Unwinding Polar Jet Observed by the Solar Dynamic Observatory/Atmospheric Imaging Assembly. *Astrophys. J. Lett.* **735**, L43.
3. Shibata K, Nitta N, Strong KT, Matsumoto R, Yokoyama T, Hirayama T, Hudson H, Ogawara Y. 1994 A gigantic coronal jet ejected from a compact active region in a coronal hole. *Astrophys. J. Lett.* **431**, L51–L53.
4. Shimojo M, Shibata K. 2000 Physical Parameters of Solar X-Ray Jets. *Astrophys. J.* **542**, 1100–1108.
5. Paraschiv AR, Bemporad A, Sterling AC. 2015 Physical properties of solar polar jets. A statistical study with Hinode XRT data. *Astron. Astrophys.* **579**, A96.
6. Brueckner GE, Bartoe JDF. 1983 Observations of high-energy jets in the corona above the quiet sun, the heating of the corona, and the acceleration of the solar wind. *Astrophys. J.* **272**, 329–348.

7. Cirtain JW, Golub L, Lundquist L, van Ballegooijen A, Savcheva A, Shimojo M, DeLuca E, Tsuneta S, Sakao T, Reeves K, et al.. 2007 Evidence for Alfvén Waves in Solar X-ray Jets. *Science* **318**, 1580.
8. Tian H, DeLuca EE, Cranmer SR, De Pontieu B, Peter H, Martínez-Sykora J, Golub L, McKillop S, Reeves KK, Miralles MP, et al.. 2014 Prevalence of small-scale jets from the networks of the solar transition region and chromosphere. *Science* **346**, 1255711.
9. Samanta T, Tian H, Yurchyshyn V, Peter H, Cao W, Sterling A, Erdélyi R, Ahn K, Feng S, Utz D, et al.. 2019 Generation of solar spicules and subsequent atmospheric heating. *Science* **366**, 890–894.
10. Hansteen VH, De Pontieu B, Rouppe van der Voort L, van Noort M, Carlsson M. 2006 Dynamic Fibrils Are Driven by Magnetoacoustic Shocks. *Astrophys. J. Lett.* **647**, L73–L76.
11. De Pontieu B, Hansteen VH, Rouppe van der Voort L, van Noort M, Carlsson M. 2007 High-Resolution Observations and Modeling of Dynamic Fibrils. *Astrophys. J.* **655**, 624–641.
12. Tian H, Yurchyshyn V, Peter H, Solanki SK, Young PR, Ni L, Cao W, Ji K, Zhu Y, Zhang J, et al.. 2018 Frequently Occurring Reconnection Jets from Sunspot Light Bridges. *Astrophys. J.* **854**, 92.
13. Sterling AC, Moore RL, Samanta T, Yurchyshyn V. 2020 Possible Production of Solar Spicules by Microfilament Eruptions. *Astrophys. J. Lett.* **893**, L45.
14. Beckers JM. 1968 Solar Spicules (Invited Review Paper). *Solar Phys.* **3**, 367–433.
15. Beckers JM. 1972 Solar Spicules. *Annu. Rev. Astron. Astrophys.* **10**, 73.
16. Sterling AC. 2000 Solar Spicules: A Review of Recent Models and Targets for Future Observations - (Invited Review). *Solar Phys.* **196**, 79–111.
17. Newton HW. 1942 Characteristic radial motions of Hα absorption markings seen with bright eruptions on the Sun's disc. *Mon. Not. Roy. Astron. Soc.* **102**, 2.
18. Kleczek J, Křivský L. 1960 Solar Limb Surges accompanied by X-Ray Emission. *Nature* **186**, 1035–1036.
19. Malville JM. 1961 Trajectories of Chromospheric Disk Surges. *Nature* **190**, 995.
20. Rust DM. 1968 Chromospheric Explosions and Satellite Sunspots. In Kiepenheuer KO, editor, *Structure and Development of Solar Active Regions* vol. 35*IAU Symposium* p. 77.
21. Roy JR. 1973 The Magnetic Properties of Solar Surges. *Solar Phys.* **28**, 95–114.
22. Ogawara Y, Acton LW, Bentley RD, Bruner ME, Culhane JL, Hiei E, Hirayama T, Hudson HS, Kosugi T, Lemen JR, et al.. 1992 The Status of YOHKOH in Orbit: an Introduction to the Initial Scientific Results. *Pub. Astron. Soc. Japan* **44**, L41–L44.
23. Domingo V, Fleck B, Poland AI. 1995 The SOHO Mission: an Overview. *Solar Phys.* **162**, 1–37.
24. Handy BN, Acton LW, Kankelborg CC, Wolfson CJ, Akin DJ, Bruner ME, Caravalho R, Catura RC, Chevalier R, Duncan DW, et al.. 1999 The transition region and coronal explorer. *Solar Phys.* **187**, 229–260.
25. Lin RP, Dennis BR, Hurford GJ, Smith DM, Zehnder A, Harvey PR, Curtis DW, Pankow D, Turin P, Bester M, et al.. 2002 The Reuven Ramaty High-Energy Solar Spectroscopic Imager (RHESSI). *Solar Phys.* **210**, 3–32.
26. Kosugi T, Matsuzaki K, Sakao T, Shimizu T, Sone Y, Tachikawa S, Hashimoto T, Minesugi K, Ohnishi A, Yamada T, et al.. 2007 The Hinode (Solar-B) Mission: An Overview. *Solar Phys.* **243**, 3–17.
27. Kaiser ML, Kucera TA, Davila JM, St. Cyr OC, Guhathakurta M, Christian E. 2008 The STEREO Mission: An Introduction. *Space Sci. Rev.* **136**, 5–16.
28. Pesnell WD, Thompson BJ, Chamberlin PC. 2012 The Solar Dynamics Observatory (SDO). *Solar Phys.* **275**, 3–15.
29. De Pontieu B, Title AM, Lemen JR, Kushner GD, Akin DJ, Allard B, Berger T, Boerner P, Cheung M, Chou C, et al.. 2014 The Interface Region Imaging Spectrograph (IRIS). *Solar Phys.* **289**, 2733–2779.
30. Scharmer GB, Bjelksjo K, Korhonen TK, Lindberg B, Petterson B. 2003 pp. 341–350. In *The 1-meter Swedish solar telescope*, vol. 4853, *Society of Photo-Optical Instrumentation Engineers (SPIE) Conference Series* pp. 341–350.
31. Cao W, Gorceix N, Coulter R, Ahn K, Rimmele TR, Goode PR. 2010 Scientific instrumentation for the 1.6 m New Solar Telescope in Big Bear. *Astronomische Nachrichten* **331**, 636.
32. Liu Z, Xu J, Gu BZ, Wang S, You JQ, Shen LX, Lu RW, Jin ZY, Chen LF, Lou K, et al.. 2014 New vacuum solar telescope and observations with high resolution. *Research in Astronomy and Astrophysics* **14**, 705–718.

33. Raouafi NE, Patsourakos S, Pariat E, Young PR, Sterling AC, Savcheva A, Shimojo M, Moreno-Insertis F, DeVore CR, Archontis V, et al.. 2016 Solar Coronal Jets: Observations, Theory, and Modeling. *Space Sci. Rev.* **201**, 1–53.
34. Ni L, Lin J, Roussev II, Schmieder B. 2016 Heating Mechanisms in the Low Solar Atmosphere through Magnetic Reconnection in Current Sheets. *Astrophys. J.* **832**, 195.
35. Ye J, Shen C, Raymond JC, Lin J, Ziegler U. 2019 Numerical study of the cascading energy conversion of the reconnection current sheet in solar eruptions. *Mon. Not. Roy. Astron. Soc.* **482**, 588–605.
36. Sterling AC, Moore RL, Falconer DA, Adams M. 2015 Small-scale filament eruptions as the driver of X-ray jets in solar coronal holes. *Nature* **523**, 437–440.
37. Sterling AC, Moore RL, Panesar NK. 2018 Magnetic Flux Cancelation as the Buildup and Trigger Mechanism for CME-producing Eruptions in Two Small Active Regions. *Astrophys. J.* **864**, 68.
38. Panesar NK, Sterling AC, Moore RL, Winebarger AR, Tiwari SK, Savage SL, Golub LE, Rachmeler LA, Kobayashi K, Brooks DH, et al.. 2019 Hi-C 2.1 Observations of Jetlet-like Events at Edges of Solar Magnetic Network Lanes. *Astrophys. J. Lett.* **887**, L8.
39. Sterling AC, Moore RL, Panesar NK, Reardon KP, Molnar M, Rachmeler LA, Savage SL, Winebarger AR. 2020 Hi-C 2.1 Observations of Small-scale Miniature-filament-eruption-like Cool Ejections in an Active Region Plage. *Astrophys. J.* **889**, 187.
40. Shibata K, Shimojo M, Yokoyama T, Ohyama M. 1996 Theory and observations of X-ray jets.. In Bentley RD, Mariska JT, editors, *Astronomical Society of the Pacific Conference Series* vol. 111*Astronomical Society of the Pacific Conference Series* pp. 29–38.
41. Tsiropoula G, Tziotziou K, Kontogiannis I, Madjarska MS, Doyle JG, Suematsu Y. 2012 Solar Fine-Scale Structures. I. Spicules and Other Small-Scale, Jet-Like Events at the Chromospheric Level: Observations and Physical Parameters. *Space Sci. Rev.* **169**, 181–244.
42. Innes DE, Bučík R, Guo LJ, Nitta N. 2016 Observations of solar X-ray and EUV jets and their related phenomena. *Astronomische Nachrichten* **337**, 1024.
43. Shen Y, Qu Z, Yuan D, Chen H, Duan Y, Zhou C, Tang Z, Huang J, Liu Y. 2019 Stereoscopic Observations of an Erupting Mini-filament-driven Two-sided-loop Jet and the Applications for Diagnosing a Filament Magnetic Field. *Astrophys. J.* **883**, 104.
44. Shibata K, Nitta N, Matsumoto R, Tajima T, Yokoyama T, Hirayama T, Hudson H. 1994 Two Types of Interaction Between Emerging Flux and Coronal Magnetic Field. In Uchida Y, Watanabe T, Shibata K, Hudson HS, editors, *X-ray solar physics from Yohkoh* p. 29.
45. Hou YJ, Li T, Zhang J. 2016 Flux rope proxies and fan-spine structures in active region NOAA 11897. *Astron. Astrophys.* **592**, A138.
46. Tian Z, Liu Y, Shen Y, Elmhamdi A, Su J, Liu YD, Kordi AS. 2017 Successive Two-sided Loop Jets Caused by Magnetic Reconnection between Two Adjacent Filamentary Threads. *Astrophys. J.* **845**, 94.
47. Zheng R, Chen Y, Huang Z, Wang B, Song H, Ning H. 2018 Two-sided-loop Jets Associated with Magnetic Reconnection between Emerging Loops and Twisted Filament Threads. *Astrophys. J.* **861**, 108.
48. Cai Q, Shen C, Ni L, Reeves KK, Kang K, Lin J. 2019 Multiband Study of a Bidirectional Jet Occurred in the Upper Chromosphere. *Journal of Geophysical Research: Space Physics* **124**, 9824–9846.
49. Sterling AC, Harra LK, Moore RL, Falconer DA. 2019 A Two-sided Loop X-Ray Solar Coronal Jet Driven by a Minifilament Eruption. *Astrophys. J.* **871**, 220.
50. Masson S, Pariat E, Aulanier G, Schrijver CJ. 2009 The Nature of Flare Ribbons in Coronal Null-Point Topology. *Astrophys. J.* **700**, 559–578.
51. Lau YT, Finn JM. 1990 Three-dimensional Kinematic Reconnection in the Presence of Field Nulls and Closed Field Lines. *Astrophys. J.* **350**, 672.
52. Li H, Jiang Y, Yang J, Yang B, Xu Z, Hong J, Bi Y. 2017 Rotating Magnetic Structures Associated with a Quasi-circular Ribbon Flare. *Astrophys. J.* **836**, 235.
53. Li T, Yang S, Zhang Q, Hou Y, Zhang J. 2018 Two Episodes of Magnetic Reconnections during a Confined Circular-ribbon Flare. *Astrophys. J.* **859**, 122.
54. Yang S, Zhang J. 2018 Mini-filament Eruptions Triggering Confined Solar Flares Observed by ONSET and SDO. *Astrophys. J. Lett.* **860**, L25.
55. Shen Y, Qu Z, Zhou C, Duan Y, Tang Z, Yuan D. 2019 Round-trip Slipping Motion of the Circular Flare Ribbon Evidenced in a Fan-spine Jet. *Astrophys. J. Lett.* **885**, L11.

56. Hou Y, Li T, Yang S, Zhang J. 2019 A Secondary Fan-spine Magnetic Structure in Active Region 11897. *Astrophys. J.* **871**, 4.
57. Yang S, Zhang Q, Xu Z, Zhang J, Zhong Z, Guo Y. 2020a Imaging and Spectral Study on the Null Point of a Fan-spine Structure During a Solar Flare. *Astrophys. J.* **898**, 101.
58. Yang J, Hong J, Li H, Jiang Y. 2020b Two Episodes of a Filament Eruption from a Fan-spine Magnetic Configuration. *Astrophys. J.* **900**, 158.
59. Huang Z, Zhang Q, Xia L, Li B, Wu Z, Fu H. 2020 Heating at the Remote Footpoints as a Brake on Jet Flows along Loops in the Solar Atmosphere. *Astrophys. J.* **897**, 113.
60. Li T, Hou Y, Zhang J, Xiang Y. 2020 NVST observations of collision-induced apparent fan-shaped jets. *Mon. Not. Roy. Astron. Soc.* **492**, 2510–2516.
61. Nisticò G, Bothmer V, Patsourakos S, Zimbardo G. 2009 Characteristics of EUV Coronal Jets Observed with STEREO/SECCHI. *Solar Phys.* **259**, 87–108.
62. Shen Y, Liu Y, Su J, Deng Y. 2012 On a Coronal Blowout Jet: The First Observation of a Simultaneously Produced Bubble-like CME and a Jet-like CME in a Solar Event. *Astrophys. J.* **745**, 164.
63. Moore RL, Cirtain JW, Sterling AC, Falconer DA. 2010 Dichotomy of Solar Coronal Jets: Standard Jets and Blowout Jets. *Astrophys. J.* **720**, 757–770.
64. Moore RL, Sterling AC, Falconer DA, Robe D. 2013 The Cool Component and the Dichotomy, Lateral Expansion, and Axial Rotation of Solar X-Ray Jets. *Astrophys. J.* **769**, 134.
65. Moore RL, Sterling AC, Panesar NK. 2018 Onset of the Magnetic Explosion in Solar Polar Coronal X-Ray Jets. *Astrophys. J.* **859**, 3.
66. Panesar NK, Sterling AC, Moore RL, Chakrapani P. 2016 Magnetic Flux Cancelation as the Trigger of Solar Quiet-region Coronal Jets. *Astrophys. J. Lett.* **832**, L7.
67. Panesar NK, Sterling AC, Moore RL. 2017 Magnetic Flux Cancellation as the Origin of Solar Quiet-region Pre-jet Minifilaments. *Astrophys. J.* **844**, 131.
68. Panesar NK, Sterling AC, Moore RL. 2018 Magnetic Flux Cancelation as the Trigger of Solar Coronal Jets in Coronal Holes. *Astrophys. J.* **853**, 189.
69. Shen Y, Liu YD, Su J, Qu Z, Tian Z. 2017 On a Solar Blowout Jet: Driving Mechanism and the Formation of Cool and Hot Components. *Astrophys. J.* **851**, 67.
70. Yang JY, Jiang YC, Yang D, Bi Y, Yang B, Zheng RS, Hong JC. 2012a The surge-like eruption of a miniature filament. *Research in Astronomy and Astrophysics* **12**, 300–312.
71. Yang J, Jiang Y, Yang B, Hong J, Yang D, Bi Y, Zheng R, Li H. 2012b A blowout surge from the eruption of a miniature filament confined by large coronal loops. *New Astron.* **17**, 732–738.
72. Zheng R, Jiang Y, Yang J, Bi Y, Hong J, Yang B, Yang D. 2013 An Extreme-ultraviolet Wave Associated with a Surge. *Astrophys. J.* **764**, 70.
73. Adams M, Sterling AC, Moore RL, Gary GA. 2014 A Small-scale Eruption Leading to a Blowout Macrospicule Jet in an On-disk Coronal Hole. *Astrophys. J.* **783**, 11.
74. Hong J, Jiang Y, Yang J, Bi Y, Li H, Yang B, Yang D. 2014 Coronal Bright Points Associated with Minifilament Eruptions. *Astrophys. J.* **796**, 73.
75. Li X, Yang S, Chen H, Li T, Zhang J. 2015 Trigger of a Blowout Jet in a Solar Coronal Mass Ejection Associated with a Flare. *Astrophys. J. Lett.* **814**, L13.
76. Hong J, Jiang Y, Yang J, Yang B, Xu Z, Xiang Y. 2016 Mini-filament Eruption as the Initiation of a Jet along Coronal Loops. *Astrophys. J.* **830**, 60.
77. Sterling AC, Moore RL. 2016 A Microfilament-eruption Mechanism for Solar Spicules. *Astrophys. J. Lett.* **828**, L9.
78. Sterling AC, Moore RL, Falconer DA, Panesar NK, Akiyama S, Yashiro S, Gopalswamy N. 2016 Minifilament Eruptions that Drive Coronal Jets in a Solar Active Region. *Astrophys. J.* **821**, 100.
79. Zhang QM, Li D, Ning ZJ, Su YN, Ji HS, Guo Y. 2016 Explosive Chromospheric Evaporation in a Circular-ribbon Flare. *Astrophys. J.* **827**, 27.
80. Hong J, Jiang Y, Yang J, Li H, Xu Z. 2017 Minifilament Eruption as the Source of a Blowout Jet, C-class Flare, and Type-III Radio Burst. *Astrophys. J.* **835**, 35.
81. Zhang Y, Zhang J. 2017 Cusp-shaped Structure of a Jet Observed By IRIS and SDO. *Astrophys. J.* **834**, 79.
82. Li H, Jiang Y, Yang J, Qu Z, Yang B, Xu Z, Bi Y, Hong J, Chen H. 2017 Blowout Surge due to Interaction between a Solar Filament and Coronal Loops. *Astrophys. J. Lett.* **842**, L20.
83. Li H, Yang J, Jiang Y, Bi Y, Qu Z, Chen H. 2018 The surge-like eruption of a miniature filament associated with circular flare ribbon. *Astrophys. Space Sci.* **363**, 26.

84. Joshi NC, Nishizuka N, Filippov B, Magara T, Tlatov AG. 2018 Flux rope breaking and formation of a rotating blowout jet. *Mon. Not. Roy. Astron. Soc.* **476**, 1286–1298.
85. Yang B, Yang J, Bi Y, Xu Z, Hong J, Li H, Chen H. 2019 Recurrent Two-sided Loop Jets Caused By Magnetic Reconnection between Erupting Minifilaments and a nearby Large Filament. *Astrophys. J.* **887**, 220.
86. Wei H, Huang Z, Hou Z, Qi Y, Fu H, Li B, Xia L. 2020 How eruptions of a small filament feed materials to a nearby larger-scaled filament. *Mon. Not. Roy. Astron. Soc.* **498**, L104–L108.
87. Tian Z, Shen Y, Liu Y. 2018 Formation and eruption of a double-decker filament triggered by micro-bursts and recurrent jets in the filament channel. *New Astron.* **65**, 7–15.
88. Canfield RC, Reardon KP, Leka KD, Shibata K, Yokoyama T, Shimojo M. 1996 H alpha Surges and X-Ray Jets in AR 7260. *Astrophys. J.* **464**, 1016.
89. Chen HD, Jiang YC, Ma SL. 2008 Observations of Hα surges and ultraviolet jets above satellite sunspots. *Astron. Astrophys.* **478**, 907–913.
90. Zhang J, Wang J, Liu Y. 2000 An Hβ surge and X-ray jet - Magnetic properties and velocity patterns. *Astron. Astrophys.* **361**, 759–765.
91. Yang LH, Jiang YC, Yang JY, Bi Y, Zheng RS, Hong JC. 2011 Observations of EUV and soft X-ray recurring jets in an active region. *Research in Astronomy and Astrophysics* **11**, 1229–1242.
92. Chen J, Su J, Yin Z, Priya TG, Zhang H, Liu J, Xu H, Yu S. 2015 Recurrent Solar Jets Induced by a Satellite Spot and Moving Magnetic Features. *Astrophys. J.* **815**, 71.
93. Sakaue T, Tei A, Asai A, Ueno S, Ichimoto K, Shibata K. 2017 Observational study on the fine structure and dynamics of a solar jet. I. Energy build-up process around a satellite spot. *Pub. Astron. Soc. Japan* **69**, 80.
94. Shen Y, Liu Y, Liu YD, Su J, Tang Z, Miao Y. 2018 Homologous Large-amplitude Nonlinear Fast-mode Magnetosonic Waves Driven by Recurrent Coronal Jets. *Astrophys. J.* **861**, 105.
95. Wang J, Li W, Denker C, Lee C, Wang H, Goode PR, McAllister A, Martin SF. 2000 Minifilament Eruption on the Quiet Sun. I. Observations at Hα Central Line. *Astrophys. J.* **530**, 1071–1084.
96. Chen H, Jiang Y, Ma S. 2009 An EUV Jet and Hα Filament Eruption Associated with Flux Cancelation in a Decaying Active Region. *Solar Phys.* **255**, 79–90.
97. Kumar P, Karpen JT, Antiochos SK, Wyper PF, DeVore CR, DeForest CE. 2019 Multiwavelength Study of Equatorial Coronal-hole Jets. *Astrophys. J.* **873**, 93.
98. Panesar NK, Moore RL, Sterling AC. 2020 Onset of Magnetic Explosion in Solar Coronal Jets in Quiet Regions on the Central Disk. *Astrophys. J.* **894**, 104.
99. Chen H, Hong J, Yang B, Xu Z, Yang J. 2020 High-resolution Chromospheric Observations of a Solar Minifilament: Formation and Destabilization. *Astrophys. J.* **902**, 8.
100. Raouafi NE, Georgoulis MK, Rust DM, Bernasconi PN. 2010 Micro-sigmoids as Progenitors of Coronal Jets: Is Eruptive Activity Self-similarly Multi-scaled?. *Astrophys. J.* **718**, 981–987.
101. Li D, Ning Z. 2012 UV1600 bright points and magnetic bipoles in solar quiet regions. *Astrophys. Space Sci.* **341**, 215–224.
102. Madjarska MS. 2019 Coronal bright points. *Living Reviews in Solar Physics* **16**, 2.
103. Moore RL, Tang F, Bohlin JD, Golub L. 1977 Halpha macrospicules: identification with EUV macrospicules and with flares in X-ray bright points.. *Astrophys. J.* **218**, 286–290.
104. Li D, Ning Z, Su Y. 2016 The bi-directional moving structures in a coronal bright point. *Astrophys. Space Sci.* **361**, 301.
105. Li D, Ning ZJ, Wang JF. 2013 Statistical study of UV bright points and magnetic elements from SDO observations. *New Astron.* **23**, 19–26.
106. Shibata K, Ishido Y, Acton LW, Strong KT, Hirayama T, Uchida Y, McAllister AH, Matsumoto R, Tsuneta S, Shimizu T, et al.. 1992 Observations of X-ray jets with the YOHKOH Soft X-ray Telescope. *Pub. Astron. Soc. Japan* **44**, L173–L179.
107. Culhane L, Harra LK, Baker D, van Driel-Gesztelyi L, Sun J, Doschek GA, Brooks DH, Lundquist LL, Kamio S, Young PR, Hansteen VH. 2007 Hinode EUV Study of Jets in the Sun's South Polar Corona. *Pub. Astron. Soc. Japan* **59**, S751.
108. Kamio S, Curdt W, Teriaca L, Innes DE. 2011 Evolution of microflares associated with bright points in coronal holes and in quiet regions. *Astron. Astrophys.* **529**, A21.
109. Chesny DL, Oluseyi HM, Orange NB, Champey PR. 2015 Quiet-Sun Network Bright Point Phenomena with Sigmoidal Signatures. *Astrophys. J.* **814**, 124.
110. Mou C, Madjarska MS, Galsgaard K, Xia L. 2018 Eruptions from quiet Sun coronal bright points. I. Observations. *Astron. Astrophys.* **619**, A55.
111. Rust DM, Kumar A. 1996 Evidence for Helically Kinked Magnetic Flux Ropes in Solar Eruptions. *Astrophys. J. Lett.* **464**, L199.

112. Canfield RC, Hudson HS, Pevtsov AA. 2000 Sigmoids as precursors of solar eruptions. *IEEE Transactions on Plasma Science* **28**, 1786–1794.
113. Brown DS, Parnell CE, Deluca EE, Golub L, McMullen RA. 2001 The Magnetic Structure of a Coronal X-Ray Bright Point. *Solar Phys.* **201**, 305–321.
114. Liu J, Fang F, Wang Y, McIntosh SW, Fan Y, Zhang Q. 2016 On the Observation and Simulation of Solar Coronal Twin Jets. *Astrophys. J.* **817**, 126.
115. Alexander D, Fletcher L. 1999 High-resolution Observations of Plasma Jets in the Solar Corona. *Solar Phys.* **190**, 167–184.
116. Ko YK, Raymond JC, Gibson SE, Alexander D, Strachan L, Holzer T, Gilbert H, Cyr OCS, Thompson BJ, Pike CD, et al.. 2005 Multialtitude Observations of a Coronal Jet during the Third Whole Sun Month Campaign. *Astrophys. J.* **623**, 519–539.
117. Jiang YC, Chen HD, Li KJ, Shen YD, Yang LH. 2007 The Hα surges and EUV jets from magnetic flux emergences and cancellations. *Astron. Astrophys.* **469**, 331–337.
118. Kirshner RP, Noyes RW. 1971 Extreme-Ultraviolet Observations of a Surge. *Solar Phys.* **20**, 428–437.
119. Schmieder B, Mein P, Vial JC, Tandberg-Hanssen E. 1983 Dynamics of a surge observed in the C IV and H alpha lines. *Astron. Astrophys.* **127**, 337–344.
120. Schmieder B, Mein P, Simnett GM, Tandberg-Hanssen E. 1988 An example of the association of X-ray and UV emission with H-alpha surges. *Astron. Astrophys.* **201**, 327–338.
121. Mulay SM, Del Zanna G, Mason H. 2017 Cool and hot emission in a recurring active region jet. *Astron. Astrophys.* **606**, A4.
122. Joshi B, Thalmann JK, Mitra PK, Chandra R, Veronig AM. 2017 Observational and Model Analysis of a Two-ribbon Flare Possibly Induced by a Neighboring Blowout Jet. *Astrophys. J.* **851**, 29.
123. Chae J, Qiu J, Wang H, Goode PR. 1999 Extreme-Ultraviolet Jets and Hα Surges in Solar Microflares. *Astrophys. J. Lett.* **513**, L75–L78.
124. Liu Y, Kurokawa H. 2004 On a Surge: Properties of an Emerging Flux Region. *Astrophys. J.* **610**, 1136–1147.
125. Schmieder B, Golub L, Antiochos SK. 1994 Comparison between cool and hot plasma behaviors of surges. *Astrophys. J.* **425**, 326–330.
126. Kayshap P, Srivastava AK, Murawski K. 2013 The Kinematics and Plasma Properties of a Solar Surge Triggered by Chromospheric Activity in AR11271. *Astrophys. J.* **763**, 24.
127. Lee KS, Innes DE, Moon YJ, Shibata K, Lee JY, Park YD. 2013 Fast Extreme-ultraviolet Dimming Associated with a Coronal Jet Seen in Multi-wavelength and Stereoscopic Observations. *Astrophys. J.* **766**, 1.
128. Dobrzycka D, Raymond JC, Cranmer SR. 2000 Ultraviolet Spectroscopy of Polar Coronal Jets. *Astrophys. J.* **538**, 922–931.
129. Yokoyama T, Shibata K. 1995 Magnetic reconnection as the origin of X-ray jets and Hα surges on the Sun. *Nature* **375**, 42–44.
130. Nishizuka N, Shimizu M, Nakamura T, Otsuji K, Okamoto TJ, Katsukawa Y, Shibata K. 2008 Giant Chromospheric Anemone Jet Observed with Hinode and Comparison with Magnetohydrodynamic Simulations: Evidence of Propagating Alfvén Waves and Magnetic Reconnection. *Astrophys. J. Lett.* **683**, L83.
131. Poisson M, Bustos C, López Fuentes M, Mand rini CH, Cristiani GD. 2020 Two successive partial mini-filament confined ejections. *Advances in Space Research* **65**, 1629–1640.
132. Singh KAP, Isobe H, Nishizuka N, Nishida K, Shibata K. 2012 Multiple Plasma Ejections and Intermittent Nature of Magnetic Reconnection in Solar Chromospheric Anemone Jets. *Astrophys. J.* **759**, 33.
133. Zhang QM, Ji HS. 2014 Blobs in recurring extreme-ultraviolet jets. *Astron. Astrophys.* **567**, A11.
134. Zhang QM, Ji HS, Su YN. 2016 Observations of Multiple Blobs in Homologous Solar Coronal Jets in Closed Loop. *Solar Phys.* **291**, 859–876.
135. Zhang QM, Ni L. 2019 Subarcsecond Blobs in Flare-related Coronal Jets. *Astrophys. J.* **870**, 113.
136. Kumar P, Cho KS. 2013 Simultaneous EUV and radio observations of bidirectional plasmoids ejection during magnetic reconnection. *Astron. Astrophys.* **557**, A115.
137. Sakaue T, Tei A, Asai A, Ueno S, Ichimoto K, Shibata K. 2018 Observational study on the fine structure and dynamics of a solar jet. II. Energy release process revealed by spectral analysis. *Pub. Astron. Soc. Japan* **70**, 99.

138. Hong J, Yang J, Chen H, Bi Y, Yang B, Chen H. 2019 Observation of a Reversal of Breakout Reconnection Preceding a Jet: Evidence of Oscillatory Magnetic Reconnection?. *Astrophys. J.* **874**, 146.
139. Li H, Yang J. 2019 A Fan Spine Jet: Nonradial Filament Eruption and the Plasmoid Formation. *Astrophys. J.* **872**, 87.
140. Yokoyama T, Shibata K. 1996 Numerical Simulation of Solar Coronal X-Ray Jets Based on the Magnetic Reconnection Model. *Pub. Astron. Soc. Japan* **48**, 353–376.
141. Yang L, He J, Peter H, Tu C, Zhang L, Feng X, Zhang S. 2013 Numerical Simulations of Chromospheric Anemone Jets Associated with Moving Magnetic Features. *Astrophys. J.* **777**, 16.
142. Ni L, Zhang QM, Murphy NA, Lin J. 2017 Blob Formation and Ejection in Coronal Jets due to the Plasmoid and Kelvin-Helmholtz Instabilities. *Astrophys. J.* **841**, 27.
143. Zhao TL, Ni L, Lin J, Ziegler U. 2018 Numerical studies of the Kelvin-Hemholtz instability in a coronal jet. *Research in Astronomy and Astrophysics* **18**, 045.
144. Archontis V, Galsgaard K, Moreno-Insertis F, Hood AW. 2006 Three-dimensional Plasmoid Evolution in the Solar Atmosphere. *Astrophys. J. Lett.* **645**, L161–L164.
145. Moreno-Insertis F, Galsgaard K. 2013 Plasma Jets and Eruptions in Solar Coronal Holes: A Three-dimensional Flux Emergence Experiment. *Astrophys. J.* **771**, 20.
146. Wyper PF, DeVore CR, Karpen JT, Lynch BJ. 2016 Three-Dimensional Simulations of Tearing and Intermittency in Coronal Jets. *Astrophys. J.* **827**, 4.
147. Mishin VV, Tomozov VM. 2016 Kelvin-Helmholtz Instability in the Solar Atmosphere, Solar Wind and Geomagnetosphere. *Solar Phys.* **291**, 3165–3184.
148. Ofman L, Thompson BJ. 2011 SDO/AIA Observation of Kelvin-Helmholtz Instability in the Solar Corona. *The Astrophysical Journal* **734**, L11.
149. Foullon C, Verwichte E, Nykyri K, Aschwanden MJ, Hannah IG. 2013 Kelvin-Helmholtz Instability of the CME Reconnection Outflow Layer in the Low Corona. *The Astrophysical Journal* **767**, 170.
150. Li D, Shen Y, Ning Z, Zhang Q, Zhou T. 2018 Two Kinds of Dynamic Behavior in a Quiescent Prominence Observed by the NVST. *The Astrophysical Journal* **863**, 192.
151. Feng L, Inhester B, Gan WQ. 2013 Kelvin-Helmholtz Instability of a Coronal Streamer. *Astrophys. J.* **774**, 141.
152. Li X, Zhang J, Yang S, Hou Y, Erdélyi R. 2018 Observing Kelvin–Helmholtz instability in solar blowout jet. *Scientific Reports* **8**, 8136.
153. Yuan D, Shen Y, Liu Y, Li H, Feng X, Keppens R. 2019 Multilayered Kelvin–Helmholtz Instability in the Solar Corona. *The Astrophysical Journal* **884**, L51.
154. Bogdanova M, Zhelyazkov I, Joshi R, Chandra R. 2018 Solar jet on 2014 April 16 modeled by Kelvin-Helmholtz instability. *New Astron.* **63**, 75–87.
155. Solanki R, Srivastava AK, Rao YK, Dwivedi BN. 2019 Twin CME Launched by a Blowout Jet Originated from the Eruption of a Quiet-Sun Mini-filament. *Solar Phys.* **294**, 68.
156. Zaqarashvili TV, Zhelyazkov I, Ofman L. 2015 Stability of Rotating Magnetized Jets in the Solar Atmosphere. I. Kelvin-Helmholtz Instability. *Astrophys. J.* **813**, 123.
157. Shimojo M, Hashimoto S, Shibata K, Hirayama T, Hudson HS, Acton LW. 1996 Statistical Study of Solar X-Ray Jets Observed with the YOHKOH Soft X-Ray Telescope. *Pub. Astron. Soc. Japan* **48**, 123–136.
158. Savcheva A, Cirtain J, Deluca EE, Lundquist LL, Golub L, Weber M, Shimojo M, Shibasaki K, Sakao T, Narukage N, et al.. 2007 A Study of Polar Jet Parameters Based on Hinode XRT Observations. *Pub. Astron. Soc. Japan* **59**, S771–S778.
159. Nishizuka N, Nakamura T, Kawate T, Singh KAP, Shibata K. 2011 Statistical Study of Chromospheric Anemone Jets Observed with Hinode/SOT. *Astrophys. J.* **731**, 43.
160. Foukal P. 1971 Morphological Relationships in the Chromospheric Hα Fine Structure. *Solar Phys.* **19**, 59–71.
161. Mulay SM, Tripathi D, Del Zanna G, Mason H. 2016 Multiwavelength study of 20 jets that emanate from the periphery of active regions. *Astron. Astrophys.* **589**, A79.
162. Paraschiv AR, Lacatus DA, Badescu T, Lupu MG, Simon S, Sandu SG, Mierla M, Rusu MV. 2010 Study of Coronal Jets During Solar Minimum Based on STEREO/SECCHI Observations. *Solar Phys.* **264**, 365–375.
163. Li LP, Zhang J, Li T, Yang SH, Zhang YZ. 2012 Study of the first productive active region in solar cycle 24. *Astron. Astrophys.* **539**, A7.

164. Wang YM, Sheeley, Jr. NR, Socker DG, Howard RA, Brueckner GE, Michels DJ, Moses D, St. Cyr OC, Llebaria A, Delaboudinière JP. 1998 Observations of Correlated White-Light and Extreme-Ultraviolet Jets from Polar Coronal Holes. *Astrophys. J.* **508**, 899–907.
165. Wang YM, Sheeley, Jr. NR. 2002 Coronal White-Light Jets near Sunspot Maximum. *Astrophys. J.* **575**, 542–552.
166. Kiss TS, Gyenge N, Erdélyi R. 2017 Systematic Variations of Macrospicule Properties Observed by SDO/AIA over Half a Decade. *Astrophys. J.* **835**, 47.
167. Pettit E. 1943 The Properties of Solar, Prominences as Related to Type.. *Astrophys. J.* **98**, 6.
168. Li X, Morgan H, Leonard D, Jeska L. 2012 A Solar Tornado Observed by AIA/SDO: Rotational Flow and Evolution of Magnetic Helicity in a Prominence and Cavity. *Astrophys. J. Lett.* **752**, L22.
169. Yang Z, Tian H, Peter H, Su Y, Samanta T, Zhang J, Chen Y. 2018 Two Solar Tornadoes Observed with the Interface Region Imaging Spectrograph. *Astrophys. J.* **852**, 79.
170. Bi Y, Jiang Y, Yang J, Zheng R, Hong J, Li H, Yang D, Yang B. 2013 Analysis of the Simultaneous Rotation and Non-radial Propagation of an Eruptive Filament. *Astrophys. J.* **773**, 162.
171. Yan XL, Xue ZK, Liu JH, Kong DF, Xu CL. 2014 Unwinding Motion of a Twisted Active Region Filament. *Astrophys. J.* **797**, 52.
172. Yang B, Jiang Y, Yang J, Hong J, Xu Z. 2015 The Formation and Eruption of a Small Circular Filament Driven by Rotating Magnetic Structures in the Quiet Sun. *Astrophys. J.* **803**, 86.
173. Bi Y, Jiang Y, Yang J, Xiang Y, Cai Y, Liu W. 2015 Partial Eruption of a Filament with Twisting Non-uniform Fields. *Astrophys. J.* **805**, 48.
174. Shen Y, Chen PF, Liu YD, Shibata K, Tang Z, Liu Y. 2019 First Unambiguous Imaging of Large-scale Quasi-periodic Extreme-ultraviolet Wave or Shock. *Astrophys. J.* **873**, 22.
175. Chen H, Yang J, Duan Y, Ji K. 2019 Observing Current Sheet Formation Forced by Non-radial Rotating Motion of Mini-filaments. *Astrophys. J.* **879**, 74.
176. Yan X, Li Q, Chen G, Xue Z, Feng L, Wang J, Yang L, Zhang Y. 2020 Dynamics Evolution of a Solar Active-region Filament from a Quasi-static State to Eruption: Rolling Motion, Untwisting Motion, Material Transfer, and Chirality. *Astrophys. J.* **904**, 15.
177. Xu Aa, Ding Jp, Yin Sy. 1984 Rotating motion in solar surges. *Chin. Astron. Astrophys.* **8**, 294–298.
178. Okten A, Cakmak H. 1990 High latitude helical surge of May 22, 1989. *Solar Phys.* **128**, 365–369.
179. Jibben P, Canfield RC. 2004 Twist Propagation in Hα Surges. *Astrophys. J.* **610**, 1129–1135.
180. Patsourakos S, Pariat E, Vourlidas A, Antiochos SK, Wuelser JP. 2008 STEREO SECCHI Stereoscopic Observations Constraining the Initiation of Polar Coronal Jets. *Astrophys. J. Lett.* **680**, L73.
181. Curdt W, Tian H, Kamio S. 2012 Explosive Events: Swirling Transition Region Jets. *Solar Phys.* **280**, 417–424.
182. Pike CD, Mason HE. 1998 Rotating Transition Region Features Observed with the SOHO Coronal Diagnostic Spectrometer. *Solar Phys.* **182**, 333–348.
183. Kamio S, Curdt W, Teriaca L, Inhester B, Solanki SK. 2010 Observations of a rotating macrospicule associated with an X-ray jet. *Astron. Astrophys.* **510**, L1.
184. Kurokawa H, Hanaoka Y, Shibata K, Uchida Y. 1987 Rotating eruption of an untwisting filament triggered by the 3B flare of 25 April, 1984. *Solar Phys.* **108**, 251–264.
185. Shibata K, Uchida Y. 1986 Sweeping-magnetic-twist mechanism for the acceleration of jets in the solar atmosphere. *Solar Phys.* **103**, 299–310.
186. Moore RL, Sterling AC, Falconer DA. 2015 Magnetic Untwisting in Solar Jets that Go into the Outer Corona in Polar Coronal Holes. *Astrophys. J.* **806**, 11.
187. Chen HD, Zhang J, Ma SL. 2012 The kinematics of an untwisting solar jet in a polar coronal hole observed by SDO/AIA. *Research in Astronomy and Astrophysics* **12**, 573–583.
188. Hong JC, Jiang YC, Yang JY, Zheng RS, Bi Y, Li HD, Yang B, Yang D. 2013 Twist in a polar blowout jet. *Research in Astronomy and Astrophysics* **13**, 253–258.
189. Yang L, Yan X, Xue Z, Li T, Wang J, Li Q, Cheng X. 2019 Transfer of Twists from a Mini-filament to Large-scale Loops by Magnetic Reconnection. *Astrophys. J.* **887**, 239.
190. Liu J, Wang Y, Erdélyi R. 2019 How Many Twists Do Solar Coronal Jets Release?. *Frontiers in Astronomy and Space Sciences* **6**, 44.
191. Liu W, Berger TE, Title AM, Tarbell TD, Low BC. 2011 Chromospheric Jet and Growing "Loop" Observed by Hinode: New Evidence of Fan-spine Magnetic Topology Resulting from Flux Emergence. *Astrophys. J.* **728**, 103.

192. Zhang QM, Ji HS. 2014 A swirling flare-related EUV jet. *Astron. Astrophys.* **561**, A134.
193. Liu J, Erdélyi R, Wang Y, Liu R. 2018 Untwisting Jets Related to Magnetic Flux Cancellation. *Astrophys. J.* **852**, 10.
194. Cheung MCM, De Pontieu B, Tarbell TD, Fu Y, Tian H, Testa P, Reeves KK, Martínez-Sykora J, Boerner P, Wülser JP, et al.. 2015 Homologous Helical Jets: Observations By IRIS, SDO, and Hinode and Magnetic Modeling With Data-Driven Simulations. *Astrophys. J.* **801**, 83.
195. Lu L, Feng L, Li Y, Li D, Ning Z, Gan W. 2019 Spectroscopic and Stereoscopic Observations of the Solar Jets. *Astrophys. J.* **887**, 154.
196. Kayshap P, Murawski K, Srivastava AK, Dwivedi BN. 2018 Rotating network jets in the quiet Sun as observed by IRIS. *Astron. Astrophys.* **616**, A99.
197. Shimojo M, Narukage N, Kano R, Sakao T, Tsuneta S, Shibasaki K, Cirtain JW, Lundquist LL, Reeves KK, Savcheva A. 2007 Fine Structures of Solar X-Ray Jets Observed with the X-Ray Telescope aboard Hinode. *Pub. Astron. Soc. Japan* **59**, S745–S750.
198. Chandrashekhar K, Bemporad A, Banerjee D, Gupta GR, Teriaca L. 2014 Characteristics of polar coronal hole jets. *Astron. Astrophys.* **561**, A104.
199. Liu W, Berger TE, Title AM, Tarbell TD. 2009 An Intriguing Chromospheric Jet Observed by Hinode: Fine Structure Kinematics and Evidence of Unwinding Twists. *Astrophys. J. Lett.* **707**, L37–L41.
200. Vasheghani Farahani S, Van Doorsselaere T, Verwichte E, Nakariakov VM. 2009 Propagating transverse waves in soft X-ray coronal jets. *Astron. Astrophys.* **498**, L29–L32.
201. Morton RJ, Verth G, McLaughlin JA, Erdélyi R. 2012 Determination of Sub-resolution Structure of a Jet by Solar Magnetoseismology. *Astrophys. J.* **744**, 5.
202. Chandrashekhar K, Morton RJ, Banerjee D, Gupta GR. 2014 The dynamical behaviour of a jet in an on-disk coronal hole observed with AIA/SDO. *Astron. Astrophys.* **562**, A98.
203. Schmieder B, Guo Y, Moreno-Insertis F, Aulanier G, Yelles Chaouche L, Nishizuka N, Harra LK, Thalmann JK, Vargas Dominguez S, Liu Y. 2013 Twisting solar coronal jet launched at the boundary of an active region. *Astron. Astrophys.* **559**, A1.
204. Feng L, Inhester B, Solanki SK, Wilhelm K, Wiegelmann T, Podlipnik B, Howard RA, Plunkett SP, Wuelser JP, Gan WQ. 2009 Stereoscopic Polar Plume Reconstructions from STEREO/SECCHI Images. *Astrophys. J.* **700**, 292–301.
205. Tian H, McIntosh SW, Habbal SR, He J. 2011 Observation of High-speed Outflow on Plume-like Structures of the Quiet Sun and Coronal Holes with Solar Dynamics Observatory/Atmospheric Imaging Assembly. *Astrophys. J.* **736**, 130.
206. Poletto G. 2015 Solar Coronal Plumes. *Living Reviews in Solar Physics* **12**, 7.
207. Wang YM. 1998 Network Activity and the Evaporative Formation of Polar Plumes. *Astrophys. J. Lett.* **501**, L145–L150.
208. Qi Y, Huang Z, Xia L, Li B, Fu H, Liu W, Sun M, Hou Z. 2019 On the Relation Between Transition Region Network Jets and Coronal Plumes. *Solar Phys.* **294**, 92.
209. Lites BW, Card G, Elmore DF, Holzer T, Lecinski A, Streander KV, Tomczyk S, Gurman JB. 1999 Dynamics of polar plumes observed at the 1998 February 26 eclipse. *Solar Phys.* **190**, 185–206.
210. Raouafi NE, Petrie GJD, Norton AA, Henney CJ, Solanki SK. 2008 Evidence for Polar Jets as Precursors of Polar Plume Formation. *Astrophys. J. Lett.* **682**, L137.
211. Raouafi NE, Stenborg G. 2014 Role of Transients in the Sustainability of Solar Coronal Plumes. *Astrophys. J.* **787**, 118.
212. Zirin H. 1976 Production of a short-lived filament by a surge. *Solar Phys.* **50**, 399–404.
213. Liu Y, Kurokawa H, Shibata K. 2005 Production of Filaments by Surges. *Astrophys. J. Lett.* **631**, L93–L96.
214. Luna M, Knizhnik K, Muglach K, Karpen J, Gilbert H, Kucera TA, Uritsky V. 2014 Observations and Implications of Large-amplitude Longitudinal Oscillations in a Solar Filament. *Astrophys. J.* **785**, 79.
215. Zhang QM, Li D, Ning ZJ. 2017 Simultaneous Transverse and Longitudinal Oscillations in a Quiescent Prominence Triggered by a Coronal Jet. *Astrophys. J.* **851**, 47.
216. Luna M, Karpen J. 2012 Large-amplitude Longitudinal Oscillations in a Solar Filament. *Astrophys. J. Lett.* **750**, L1.
217. Awasthi AK, Liu R, Wang Y. 2019 Double-decker Filament Configuration Revealed by Mass Motions. *Astrophys. J.* **872**, 109.
218. Shen Y, Liu YD, Chen PF, Ichimoto K. 2014 Simultaneous Transverse Oscillations of a Prominence and a Filament and Longitudinal Oscillation of Another Filament Induced by a Single Shock Wave. *Astrophys. J.* **795**, 130.

219. Pant V, Mazumder R, Yuan D, Banerjee D, Srivastava AK, Shen Y. 2016 Simultaneous Longitudinal and Transverse Oscillations in an Active-Region Filament. *Solar Phys.* **291**, 3303–3315.
220. Guo J, Liu Y, Zhang H, Deng Y, Lin J, Su J. 2010 A Flux Rope Eruption Triggered by Jets. *Astrophys. J.* **711**, 1057–1061.
221. Wang J, Yan X, Qu Z, UeNo S, Ichimoto K, Deng L, Cao W, Liu Z. 2018 Formation of an Active Region Filament Driven By a Series of Jets. *Astrophys. J.* **863**, 180.
222. Wang J, Yan X, Guo Q, Kong D, Xue Z, Yang L, Li Q. 2019 Formation and material supply of an active-region filament associated with newly emerging flux. *Mon. Not. Roy. Astron. Soc.* **488**, 3794–3803.
223. Zimovets IV, Nakariakov VM. 2015 Excitation of kink oscillations of coronal loops: statistical study. *Astron. Astrophys.* **577**, A4.
224. Shen Y, Tang Z, Li H, Liu Y. 2018 Coronal EUV, QFP, and kink waves simultaneously launched during the course of jet-loop interaction. *Mon. Not. Roy. Astron. Soc.* **480**, L63–L67.
225. Sarkar S, Pant V, Srivastava AK, Banerjee D. 2016 Transverse Oscillations in a Coronal Loop Triggered by a Jet. *Solar Phys.* **291**, 3269–3288.
226. Ma S, Raymond JC, Golub L, Lin J, Chen H, Grigis P, Testa P, Long D. 2011 Observations and Interpretation of a Low Coronal Shock Wave Observed in the EUV by the SDO/AIA. *Astrophys. J.* **738**, 160.
227. Shen Y, Liu Y. 2012a Simultaneous Observations of a Large-scale Wave Event in the Solar Atmosphere: From Photosphere to Corona. *Astrophys. J. Lett.* **752**, L23.
228. Shen Y, Liu Y. 2012b Evidence for the Wave Nature of an Extreme Ultraviolet Wave Observed by the Atmospheric Imaging Assembly on Board the Solar Dynamics Observatory. *Astrophys. J.* **754**, 7.
229. Shen Y, Liu Y, Su J, Li H, Zhao R, Tian Z, Ichimoto K, Shibata K. 2013 Diffraction, Refraction, and Reflection of an Extreme-ultraviolet Wave Observed during Its Interactions with Remote Active Regions. *Astrophys. J. Lett.* **773**, L33.
230. Mei ZX, Keppens R, Cai QW, Ye J, Xie XY, Li Y. 2020 3D numerical experiment for EUV waves caused by flux rope eruption. *Mon. Not. Roy. Astron. Soc.* **493**, 4816–4829.
231. Shen Y, Tang Z, Miao Y, Su J, Liu Y. 2018 EUV Waves Driven by the Sudden Expansion of Transequatorial Loops Caused by Coronal Jets. *Astrophys. J. Lett.* **860**, L8.
232. Li H, Feng H, Liu Y, Shen Y, Tian Z, Zhao G, Zhao A. 2020 On the Fast Propagating Ultra-hot Disturbance Captured by SDO/AIA: An In-depth Insight into the Coronal Nonlinear Dynamics. *Astrophys. J. Lett.* **898**, L8.
233. Su W, Cheng X, Ding MD, Chen PF, Sun JQ. 2015 A Type II Radio Burst without a Coronal Mass Ejection. *Astrophys. J.* **804**, 88.
234. Shen Y, Ichimoto K, Ishii TT, Tian Z, Zhao R, Shibata K. 2014 A Chain of Winking (Oscillating) Filaments Triggered by an Invisible Extreme-ultraviolet Wave. *Astrophys. J.* **786**, 151.
235. Crifo F, Picat JP, Cailloux M. 1983 Coronal Transients - Loop or Bubble. *Solar Phys.* **83**, 143–152.
236. Shen YD, Liu Y, Liu R. 2011 A time series of filament eruptions observed by three eyes from space: from failed to successful eruptions. *Research in Astronomy and Astrophysics* **11**, 594–606.
237. Shen Y, Liu Y, Su J. 2012 Sympathetic Partial and Full Filament Eruptions Observed in One Solar Breakout Event. *Astrophys. J.* **750**, 12.
238. Gilbert HR, Serex EC, Holzer TE, MacQueen RM, McIntosh PS. 2001 Narrow Coronal Mass Ejections. *Astrophys. J.* **550**, 1093–1101.
239. Liu J, Wang Y, Shen C, Liu K, Pan Z, Wang S. 2015 A Solar Coronal Jet Event Triggers a Coronal Mass Ejection. *Astrophys. J.* **813**, 115.
240. Miao Y, Liu Y, Li HB, Shen Y, Yang S, Elmhamdi A, Kordi AS, Abidin ZZ. 2018 A Blowout Jet Associated with One Obvious Extreme-ultraviolet Wave and One Complicated Coronal Mass Ejection Event. *Astrophys. J.* **869**, 39.
241. Wood BE, Karovska M, Cook JW, Howard RA, Brueckner GE. 1999 Kinematic Measurements of Polar Jets Observed by the Large-Angle Spectrometric Coronagraph. *Astrophys. J.* **523**, 444–449.
242. Zheng R, Chen Y, Du G, Li C. 2016 Solar Jet-Coronal Hole Collision and a Closely Related Coronal Mass Ejection. *Astrophys. J. Lett.* **819**, L18.
243. Duan Y, Shen Y, Chen H, Liang H. 2019 The Birth of a Jet-driven Twin CME and Its Deflection from Remote Magnetic Fields. *Astrophys. J.* **881**, 132.

244. Liu Y, Su JT, Morimoto T, Kurokawa H, Shibata K. 2005 Observations of an Emerging Flux Region Surge: Implications for Coronal Mass Ejections Triggered by Emerging Flux. *Astrophys. J.* **628**, 1056–1060.
245. Corti G, Poletto G, Suess ST, Moore RL, Sterling AC. 2007 Cool-Plasma Jets that Escape into the Outer Corona. *Astrophys. J.* **659**, 1702–1712.
246. Liu Y. 2008 A Study of Surges: II. On the Relationship between Chromospheric Surges and Coronal Mass Ejections. *Solar Phys.* **249**, 75–84.
247. Hong J, Jiang Y, Zheng R, Yang J, Bi Y, Yang B. 2011 A Micro Coronal Mass Ejection Associated Blowout Extreme-ultraviolet Jet. *Astrophys. J. Lett.* **738**, L20.
248. Chandra R, Mandrini CH, Schmieder B, Joshi B, Cristiani GD, Cremades H, Pariat E, Nuevo FA, Srivastava AK, Uddin W. 2017 Blowout jets and impulsive eruptive flares in a bald-patch topology. *Astron. Astrophys.* **598**, A41.
249. Panesar NK, Sterling AC, Moore RL. 2016 Homologous Jet-driven Coronal Mass Ejections from Solar Active Region 12192. *Astrophys. J. Lett.* **822**, L23.
250. Jiang Y, Shen Y, Yi B, Yang J, Wang J. 2008 Magnetic Interaction: A Transequatorial Jet and Interconnecting Loops. *Astrophys. J.* **677**, 699–703.
251. Liu C, Prasad A, Lee J, Wang H. 2020 An Eruptive Circular-ribbon Flare with Extended Remote Brightenings. *Astrophys. J.* **899**, 34.
252. Li H, Yang J, Hong J, Chen H. 2019 The Formation of CME from Coupling Fan-spine Magnetic System: A Difficult Journey. *Astrophys. J. Lett.* **886**, L34.
253. Alzate N, Morgan H. 2016 Jets, Coronal "Puffs," and a Slow Coronal Mass Ejection Caused by an Opposite-polarity Region within an Active Region Footpoint. *Astrophys. J.* **823**, 129.
254. Miao Y, Liu Y, Shen YD, Elmhamdi A, Kordi AS, Li HB, Abidin ZZ, Tian ZJ. 2019 A New Small Satellite Sunspot Triggering Recurrent Standard and Blowout Coronal Jets. *Astrophys. J.* **877**, 61.
255. Reames DV. 1999 Particle acceleration at the Sun and in the heliosphere. *Space Sci. Rev.* **90**, 413–491.
256. Vlahos L, Anastasiadis A, Papaioannou A, Kouloumvakos A, Isliker H. 2019 Sources of solar energetic particles. *Philosophical Transactions of the Royal Society of London Series A* **377**, 20180095.
257. Aurass H, Klein KL, Martens PCH. 1994 First detection of correlated electron beams and plasma jets in radio and soft x-ray data. *Solar Phys.* **155**, 203–206.
258. Kundu MR, Raulin JP, Nitta N, Hudson HS, Shimojo M, Shibata K, Raoult A. 1995 Detection of Nonthermal Radio Emission from Coronal X-Ray Jets. *Astrophys. J. Lett.* **447**, L135.
259. Li C, Matthews SA, van Driel-Gesztelyi L, Sun J, Owen CJ. 2011 Coronal Jets, Magnetic Topologies, and the Production of Interplanetary Electron Streams. *Astrophys. J.* **735**, 43.
260. Chen B, Bastian TS, White SM, Gary DE, Perley R, Rupen M, Carlson B. 2013 Tracing Electron Beams in the Sun's Corona with Radio Dynamic Imaging Spectroscopy. *Astrophys. J. Lett.* **763**, L21.
261. Bučík R, Innes DE, Mall U, Korth A, Mason GM, Gómez-Herrero R. 2014 Multi-spacecraft Observations of Recurrent ^{3}He-rich Solar Energetic Particles. *Astrophys. J.* **786**, 71.
262. Chen B, Yu S, Battaglia M, Farid S, Savcheva A, Reeves KK, Krucker S, Bastian TS, Guo F, Tassev S. 2018 Magnetic Reconnection Null Points as the Origin of Semirelativistic Electron Beams in a Solar Jet. *Astrophys. J.* **866**, 62.
263. Wang YM, Pick M, Mason GM. 2006 Coronal Holes, Jets, and the Origin of ^{3}He-rich Particle Events. *Astrophys. J.* **639**, 495–509.
264. Kahler SW, Reames DV, Sheeley, N. R. J. 2001 Coronal Mass Ejections Associated with Impulsive Solar Energetic Particle Events. *Astrophys. J.* **562**, 558–565.
265. Klein KL, Posner A. 2005 The onset of solar energetic particle events: prompt release of deka-MeV protons and associated coronal activity. *Astron. Astrophys.* **438**, 1029–1042.
266. Pick M, Mason GM, Wang YM, Tan C, Wang L. 2006 Solar Source Regions for ^{3}He-rich Solar Energetic Particle Events Identified Using Imaging Radio, Optical, and Energetic Particle Observations. *Astrophys. J.* **648**, 1247–1255.
267. Nitta NV, Reames DV, De Rosa ML, Liu Y, Yashiro S, Gopalswamy N. 2006 Solar Sources of Impulsive Solar Energetic Particle Events and Their Magnetic Field Connection to the Earth. *Astrophys. J.* **650**, 438–450.
268. Bučík R, Innes DE, Mason GM, Wiedenbeck ME, Gómez-Herrero R, Nitta NV. 2018 ^{3}He-rich Solar Energetic Particles in Helical Jets on the Sun. *Astrophys. J.* **852**, 76.

269. Chen Nh, Bučík R, Innes DE, Mason GM. 2015 Case studies of multi-day ^{3}He-rich solar energetic particle periods. *Astron. Astrophys.* **580**, A16.
270. Nitta NV, Mason GM, Wiedenbeck ME, Cohen CMS, Krucker S, Hannah IG, Shimojo M, Shibata K. 2008 Coronal Jet Observed by Hinode as the Source of a^{3}He-rich Solar Energetic Particle Event. *Astrophys. J. Lett.* **675**, L125.
271. Bučík R, Wiedenbeck ME, Mason GM, Gómez-Herrero R, Nitta NV, Wang L. 2018 ^{3}He-rich Solar Energetic Particles from Sunspot Jets. *Astrophys. J. Lett.* **869**, L21.
272. Reid HAS, Ratcliffe H. 2014 A review of solar type III radio bursts. *Research in Astronomy and Astrophysics* **14**, 773–804.
273. Krucker S, Kontar EP, Christe S, Glesener L, Lin RP. 2011 Electron Acceleration Associated with Solar Jets. *Astrophys. J.* **742**, 82.
274. Saint-Hilaire P, Krucker S, Christe S, Lin RP. 2009 The X-ray Detectability of Electron Beams Escaping from the Sun. *Astrophys. J.* **696**, 941–952.
275. Glesener L, Krucker S, Lin RP. 2012 Hard X-Ray Observations of a Jet and Accelerated Electrons in the Corona. *Astrophys. J.* **754**, 9.
276. Zharkova VV, Arzner K, Benz AO, Browning P, Dauphin C, Emslie AG, Fletcher L, Kontar EP, Mann G, Onofri M, et al.. 2011 Recent Advances in Understanding Particle Acceleration Processes in Solar Flares. *Space Sci. Rev.* **159**, 357–420.
277. Li Y, Lin J. 2012 Acceleration of Electrons and Protons in Reconnecting Current Sheets Including Single or Multiple X-points. *Solar Phys.* **279**, 91–113.
278. Li Y, Wu N, Lin J. 2017 Charged-particle acceleration in a reconnecting current sheet including multiple magnetic islands and a nonuniform background magnetic field. *Astron. Astrophys.* **605**, A120.
279. Parnell CE, De Moortel I. 2012 A contemporary view of coronal heating. *Philosophical Transactions of the Royal Society of London Series A* **370**, 3217–3240.
280. Geiss J, Gloeckler G, von Steiger R. 1995 Origin of the Solar Wind From Composition Data. *Space Sci. Rev.* **72**, 49–60.
281. Cranmer SR, Winebarger AR. 2019 The Properties of the Solar Corona and Its Connection to the Solar Wind. *Annu. Rev. Astron. Astrophys.* **57**, 157–187.
282. McIntosh SW. 2012 Recent Observations of Plasma and Alfvénic Wave Energy Injection at the Base of the Fast Solar Wind. *Space Sci. Rev.* **172**, 69–87.
283. Parker EN. 1988 Nanoflares and the Solar X-Ray Corona. *Astrophys. J.* **330**, 474.
284. De Pontieu B, McIntosh SW, Carlsson M, Hansteen VH, Tarbell TD, Boerner P, Martinez-Sykora J, Schrijver CJ, Title AM. 2011 The Origins of Hot Plasma in the Solar Corona. *Science* **331**, 55.
285. De Pontieu B, McIntosh SW, Carlsson M, Hansteen VH, Tarbell TD, Schrijver CJ, Title AM, Shine RA, Tsuneta S, Katsukawa Y, et al.. 2007 Chromospheric Alfvénic Waves Strong Enough to Power the Solar Wind. *Science* **318**, 1574.
286. Okamoto TJ, De Pontieu B. 2011 Propagating Waves Along Spicules. *Astrophys. J. Lett.* **736**, L24.
287. Moore RL, Sterling AC, Cirtain JW, Falconer DA. 2011 Solar X-ray Jets, Type-II Spicules, Granule-size Emerging Bipoles, and the Genesis of the Heliosphere. *Astrophys. J. Lett.* **731**, L18.
288. McIntosh SW, de Pontieu B, Carlsson M, Hansteen V, Boerner P, Goossens M. 2011a Alfvénic waves with sufficient energy to power the quiet solar corona and fast solar wind. *Nature* **475**, 477–480.
289. McIntosh SW, Leamon RJ, De Pontieu B. 2011b The Spectroscopic Footprint of the Fast Solar Wind. *Astrophys. J.* **727**, 7.
290. Tian H, McIntosh SW, Wang T, Ofman L, De Pontieu B, Innes DE, Peter H. 2012 Persistent Doppler Shift Oscillations Observed with Hinode/EIS in the Solar Corona: Spectroscopic Signatures of Alfvénic Waves and Recurring Upflows. *Astrophys. J.* **759**, 144.
291. De Moortel I, McIntosh SW, Threlfall J, Bethge C, Liu J. 2014 Potential Evidence for the Onset of Alfvénic Turbulence in Trans-equatorial Coronal Loops. *Astrophys. J. Lett.* **782**, L34.
292. Threlfall J, De Moortel I, McIntosh SW, Bethge C. 2013 First comparison of wave observations from CoMP and AIA/SDO. *Astron. Astrophys.* **556**, A124.
293. Neugebauer M, Goldstein BE, McComas DJ, Suess ST, Balogh A. 1995 Ulysses observations of microstreams in the solar wind from coronal holes. *J. Geophys. Res.* **100**, 23389–23396.
294. Neugebauer M. 2012 Evidence for Polar X-Ray Jets as Sources of Microstream Peaks in the Solar Wind. *Astrophys. J.* **750**, 50.

295. Horbury TS, Matteini L, Stansby D. 2018 Short, large-amplitude speed enhancements in the near-Sunfast solar wind. *Mon. Not. Roy. Astron. Soc.* **478**, 1980–1986.
296. Sako N, Shimojo M, Watanabe T, Sekii T. 2013 A Statistical Study of Coronal Active Events in the North Polar Region. *Astrophys. J.* **775**, 22.
297. Yu HS, Jackson BV, Buffington A, Hick PP, Shimojo M, Sako N. 2014 The Three-dimensional Analysis of Hinode Polar Jets using Images from LASCO C2, the Stereo COR2 Coronagraphs, and SMEI. *Astrophys. J.* **784**, 166.
298. Yu HS, Jackson BV, Yang YH, Chen NH, Buffington A, Hick PP. 2016 A 17 June 2011 polar jet and its presence in the background solar wind. *Journal of Geophysical Research (Space Physics)* **121**, 4985–4997.
299. Heyvaerts J, Priest ER, Rust DM. 1977 An emerging flux model for the solar phenomenon.. *Astrophys. J.* **216**, 123–137.
300. Chen PF, Shibata K. 2000 An Emerging Flux Trigger Mechanism for Coronal Mass Ejections. *Astrophys. J.* **545**, 524–531.
301. Moreno-Insertis F, Galsgaard K, Ugarte-Urra I. 2008 Jets in Coronal Holes: Hinode Observations and Three-dimensional Computer Modeling. *Astrophys. J. Lett.* **673**, L211.
302. Archontis V, Hood AW. 2013 A Numerical Model of Standard to Blowout Jets. *Astrophys. J. Lett.* **769**, L21.
303. Lee EJ, Archontis V, Hood AW. 2015 Helical Blowout Jets in the Sun: Untwisting and Propagation of Waves. *Astrophys. J. Lett.* **798**, L10.
304. Huang Z, Madjarska MS, Doyle JG, Lamb DA. 2012 Coronal hole boundaries at small scales. IV. SOT view. Magnetic field properties of small-scale transient brightenings in coronal holes. *Astron. Astrophys.* **548**, A62.
305. Young PR, Muglach K. 2014a Solar Dynamics Observatory and Hinode Observations of a Blowout Jet in a Coronal Hole. *Solar Phys.* **289**, 3313–3329.
306. Young PR, Muglach K. 2014b A coronal hole jet observed with Hinode and the Solar Dynamics Observatory. *Pub. Astron. Soc. Japan* **66**, S12.
307. Sterling AC, Moore RL, Falconer DA, Panesar NK, Martinez F. 2017 Solar Active Region Coronal Jets. II. Triggering and Evolution of Violent Jets. *Astrophys. J.* **844**, 28.
308. McGlasson RA, Panesar NK, Sterling AC, Moore RL. 2019 Magnetic Flux Cancellation as the Trigger Mechanism of Solar Coronal Jets. *Astrophys. J.* **882**, 16.
309. Pariat E, Antiochos SK, DeVore CR. 2009 A Model for Solar Polar Jets. *Astrophys. J.* **691**, 61–74.
310. Pariat E, Antiochos SK, DeVore CR. 2010 Three-dimensional Modeling of Quasi-homologous Solar Jets. *Astrophys. J.* **714**, 1762–1778.
311. Rachmeler LA, Pariat E, DeForest CE, Antiochos S, Török T. 2010 Symmetric Coronal Jets: A Reconnection-controlled Study. *Astrophys. J.* **715**, 1556–1565.
312. Pariat E, Dalmasse K, DeVore CR, Antiochos SK, Karpen JT. 2015 Model for straight and helical solar jets. I. Parametric studies of the magnetic field geometry. *Astron. Astrophys.* **573**, A130.
313. Pariat E, Dalmasse K, DeVore CR, Antiochos SK, Karpen JT. 2016 A model for straight and helical solar jets. II. Parametric study of the plasma beta. *Astron. Astrophys.* **596**, A36.
314. Karpen JT, DeVore CR, Antiochos SK, Pariat E. 2017 Reconnection-Driven Coronal-Hole Jets with Gravity and Solar Wind. *Astrophys. J.* **834**, 62.
315. Wyper PF, DeVore CR. 2016 Simulations of Solar Jets Confined by Coronal Loops. *Astrophys. J.* **820**, 77.
316. Antiochos SK, DeVore CR, Klimchuk JA. 1999 A Model for Solar Coronal Mass Ejections. *Astrophys. J.* **510**, 485–493.
317. Chen Y, Du G, Zhao D, Wu Z, Liu W, Wang B, Ruan G, Feng S, Song H. 2016 Imaging a Magnetic-breakout Solar Eruption. *Astrophys. J. Lett.* **820**, L37.
318. Wyper PF, Antiochos SK, DeVore CR. 2017 A universal model for solar eruptions. *Nature* **544**, 452–455.
319. Wyper PF, DeVore CR, Antiochos SK. 2018a A Breakout Model for Solar Coronal Jets with Filaments. *Astrophys. J.* **852**, 98.
320. Wyper PF, DeVore CR, Karpen JT, Antiochos SK, Yeates AR. 2018b A Model for Coronal Hole Bright Points and Jets Due to Moving Magnetic Elements. *Astrophys. J.* **864**, 165.
321. Kumar P, Karpen JT, Antiochos SK, Wyper PF, DeVore CR, DeForest CE. 2018 Evidence for the Magnetic Breakout Model in an Equatorial Coronal-hole Jet. *Astrophys. J.* **854**, 155.

322. Jiang C, Wu ST, Feng X, Hu Q. 2016 Data-driven magnetohydrodynamic modelling of a flux-emerging active region leading to solar eruption. *Nature Communications* **7**, 11522.
323. Nayak SS, Bhattacharyya R, Prasad A, Hu Q, Kumar S, Joshi B. 2019 A Data-constrained Magnetohydrodynamic Simulation of Successive Events of Blowout Jet and C-class Flare in NOAA AR 12615. *Astrophys. J.* **875**, 10.
324. Yang WH, Sturrock PA, Antiochos SK. 1986 Force-free Magnetic Fields: The Magneto-frictional Method. *Astrophys. J.* **309**, 383.
325. Meyer KA, Savcheva AS, Mackay DH, DeLuca EE. 2019 Nonlinear Force-free Field Modeling of Solar Coronal Jets in Theoretical Configurations. *Astrophys. J.* **880**, 62.
326. Török T, Lionello R, Titov VS, Leake JE, Mikić Z, Linker JA, Linton MG. 2016 Modeling Jets in the Corona and Solar Wind. In Dorotovic I, Fischer CE, Temmer M, editors, *Coimbra Solar Physics Meeting: Ground-based Solar Observations in the Space Instrumentation Era* vol. 504*Astronomical Society of the Pacific Conference Series* p. 185.
327. Lionello R, Török T, Titov VS, Leake JE, Mikić Z, Linker JA, Linton MG. 2016 The Contribution of Coronal Jets to the Solar Wind. *Astrophys. J. Lett.* **831**, L2.
328. Szente J, Toth G, Manchester, IV WB, van der Holst B, Landi E, Gombosi TI, DeVore CR, Antiochos SK. 2017 Coronal Jets Simulated with the Global Alfvén Wave Solar Model. *Astrophys. J.* **834**, 123.
329. Welsch BT, Fisher GH, Sun X. 2013 A Magnetic Calibration of Photospheric Doppler Velocities. *Astrophys. J.* **765**, 98.
330. Fox NJ, Velli MC, Bale SD, Decker R, Driesman A, Howard RA, Kasper JC, Kinnison J, Kusterer M, Lario D, Lockwood MK, McComas DJ, Raouafi NE, Szabo A. 2016 The Solar Probe Plus Mission: Humanity's First Visit to Our Star. *Space Sci. Rev.* **204**, 7–48.
331. Müller D, St. Cyr OC, Zouganelis I, Gilbert HR, Marsden R, Nieves-Chinchilla T, Antonucci E, Auchère F, Berghmans D, Horbury TS, Howard RA, Krucker S, Maksimovic M, Owen CJ, Rochus P, Rodriguez-Pacheco J, Romoli M, Solanki SK, Bruno R, Carlsson M, Fludra A, Harra L, Hassler DM, Livi S, Louarn P, Peter H, Schühle U, Teriaca L, del Toro Iniesta JC, Wimmer-Schweingruber RF, Marsch E, Velli M, De Groof A, Walsh A, Williams D. 2020 The Solar Orbiter mission. Science overview. *Astron. Astrophys.* **642**, A1.
332. Rast MP, Bello González N, Bellot Rubio L, Cao W, Cauzzi G, DeLuca E, De Pontieu B, Fletcher L, Gibson SE, Judge PG, Katsukawa Y, Kazachenko MD, Khomenko E, Landi E, Martínez Pillet V, Petrie GJD, Qiu J, Rachmeler LA, Rempel M, Schmidt W, Scullion E, Sun X, Welsch BT, Andretta V, Antolin P, Ayres TR, Balasubramaniam KS, Ballai I, Berger TE, Bradshaw SJ, Carlsson M, Casini R, Centeno R, Cranmer SR, DeForest C, Deng Y, Erdélyi R, Fedun V, Fischer CE, González Manrique SJ, Hahn M, Harra L, Henriques VMJ, Hurlburt NE, Jaeggli S, Jafarzadeh S, Jain R, Jefferies SM, Keys PH, Kowalski AF, Kuckein C, Kuhn JR, Liu J, Liu W, Longcope D, McAteer RTJ, McIntosh SW, McKenzie DE, Miralles MP, Morton RJ, Muglach K, Nelson CJ, Panesar NK, Parenti S, Parnell CE, Poduval B, Reardon KP, Reep JW, Schad TA, Schmit D, Sharma R, Socas-Navarro H, Srivastava AK, Sterling AC, Suematsu Y, Tarr LA, Tiwari S, Tritschler A, Verth G, Vourlidas A, Wang H, Wang YM, NSO, project D, instrument scientists D, the DKIST Science Working Group, DKIST Critical Science Plan Community t. 2020 Critical Science Plan for the Daniel K. Inouye Solar Telescope (DKIST). *arXiv e-prints* p. arXiv:2008.08203.
333. Gan WQ, Zhu C, Deng YY, Li H, Su Y, Zhang HY, Chen B, Zhang Z, Wu J, Deng L, Huang Y, Yang JF, Cui JJ, Chang J, Wang C, Wu J, Yin ZS, Chen W, Fang C, Yan YH, Lin J, Xiong WM, Chen B, Bao HC, Cao CX, Bai YP, Wang T, Chen BL, Li XY, Zhang Y, Feng L, Su JT, Li Y, Chen W, Li YP, Su YN, Wu HY, Gu M, Huang L, Tang XJ. 2019 Advanced Space-based Solar Observatory (ASO-S): an overview. *Research in Astronomy and Astrophysics* **19**, 156.